Available online at www.sciencedirect.com
ScienceDirect
Journal of Contaminant Hydrology 89 (2007) 71–106
JOURNAL OF Contaminant Hydrology
www.elsevier.com/locate/jconhyd

Transport of *Escherichia coli* bacteria through laboratory columns of glacial-outwash sediments: Estimating model parameter values based on sediment characteristics

J. Levy [a,*], K. Sun [a,1], R.H. Findlay [b,2], F.T. Farruggia [c,3], J. Porter [b,4], K.L. Mumy [b,5], J. Tomaras [b,6], A. Tomaras [b,7]

[a] *Department of Geology, Miami University, Oxford, OH 45056, USA*
[b] *Department of Microbiology, Miami University, Oxford, OH 45056, USA*
[c] *Department of Botany, Miami University, Oxford, OH 45056, USA*

Received 7 March 2005; received in revised form 4 July 2006; accepted 13 August 2006
Available online 13 November 2006

Abstract

Bacterial transport through cores of intact, glacial-outwash aquifer sediment was investigated with the overall goal of better understanding bacterial transport and developing a predictive capability based on the sediment characteristics. Variability was great among the cores. Normalized maximum bacterial-effluent concentrations ranged from 5.4×10^{-7} to 0.36 and effluent recovery ranged from 2.9×10^{-4} to 59%. Bacterial breakthrough was generally rapid with a sharp peak occurring nearly twice as early as the bromide peak. Bacterial breakthrough exhibited a long tail of relatively constant concentration averaging three orders of magnitude less than the peak concentration for up to 32 pore volumes. The tails were consistent with non-equilibrium detachment, corroborated by the results of flow interruption experiments. Bacterial breakthrough

* Corresponding author. Tel.: +1 513 529 1947; fax: +1 513 529 1542.
E-mail address: levyj@muohio.edu (J. Levy).
[1] Current address: CH2M HILL Inc., 3 Hutton Centre Drive, Suite 200, Santa Ana, CA 92707, USA.
[2] Current address: Department of Biological Sciences, University of Alabama, Tuscaloosa, AL 35487-0344, USA.
[3] Current address: School of Life Sciences, Arizona State University, Mail Code 4601, Tempe, AZ 85287, USA.
[4] Current address: Department of Earth and Environmental Sciences, Lehigh University, Bethlehem, PA 18015, USA.
[5] Current address: Department of Microbiology and Molecular Genetics, Harvard Medical School, Boston, MA 02115, USA.
[6] Current address: Environmental Science and Engineering, Colorado School of Mines, Golden, CO 80401, USA.
[7] Current address: Department of Microbiology, University of Colorado Health Sciences Center, Aurora, Colorado 80011, USA.

0169-7722/$ - see front matter
doi:10.1016/j.jconhyd.2006.08.006

was accurately simulated with a transport model incorporating advection, dispersion and first-order non-equilibrium attachment/detachment. Relationships among bacterial transport and sediment characteristics were explored with multiple regression analyses. These analyses indicated that for these cores and experimental conditions, easily-measurable sediment characteristics – median grain size, degree of sorting, organic-matter content and hydraulic conductivity – accounted for 66%, 61% and 89% of the core-to-core variability in the bacterial effective porosity, dispersivity and attachment-rate coefficient, respectively. In addition, the bacterial effective porosity, median grain size and organic-matter content accounted for 76% of the inter-core variability in the detachment-rate coefficient. The resulting regression equations allow prediction of bacterial transport based on sediment characteristics and are a possible alternative to using colloid–filtration theory. Colloid–filtration theory, used without the benefit of running bacterial transport experiments, did not as accurately replicate the observed variability in the attachment-rate coefficient.

Keywords: Bacterial transport; Sediment characteristics; Column experiments; Transport modeling; *Escherichia coli*

1. Introduction

Fecal contamination of groundwater causes numerous disease outbreaks in the US (Craun and Calderon, 1997; Macler and Merkle, 2000). World-wide, there is a substantial risk of well-water contamination when pit latrines are located within 200 m of wells (Foppen et al., 2005). *Escherichia coli* (*E. coli*), a species of coliform bacteria, are commonly used as indicators of fecal contamination due to the ease of their detection and quantification. Therefore, predicting the transport and fate of *E. coli* in a variety of geologic settings is important to assessing the likelihood of fecal contamination reaching a well.

The likelihood of allochthonous bacteria such as *E. coli* contaminating a well via transport in groundwater depends on many factors (Gerba et al., 1991; Harvey, 1991; Bitton and Harvey, 1992). The majority of previous studies used column experiments to examine the effects of individual factors on bacterial transport. These experiments focused on the effects of the bacteria themselves (Huyysman and Verstraete, 1993; McCaulou et al., 1994; Harvey et al., 1995; McCaulou et al., 1995; Weiss et al., 1995; Harvey et al., 1997), the physical and chemical properties of aquifer sediments (Fontes et al., 1991; Harvey et al., 1993; Morley et al., 1998; Fuller et al., 2000; Bolster et al., 2001; Dong et al., 2002), the presence of sediment surface coatings (Scholl and Harvey, 1992; Knapp et al., 1998; Bolster et al., 2001) and sediment organic content (Johnson and Logan, 1996). The influence of groundwater chemistry (mainly the ionic strength and pH) (Fontes et al., 1991; Scholl and Harvey, 1992; Gross and Logan, 1995; Jewett et al., 1995; Bolster et al., 2001) and hydraulic conditions (Morley et al., 1998; Hendry et al., 1999) have also been considered.

Most of these studies are not well suited for developing a practical predictive capability for two main reasons. First, most previous studies focused on the effects of individual factors on bacterial transport, and did not allow assessment of the combined effects on bacterial transport due to changes in more than one factor simultaneously. Second, most of the previous studies used columns packed with artificial aquifer material (such as commercial sand) or repacked with sieved and washed natural aquifer materials. Because artificial structures may be created during the repacking of columns (Harvey, 1997), or natural preferential pathways may be destroyed, bacteria may exhibit different transport behavior through intact natural sediment cores as compared to repacked artificial columns. Natural physical and chemical heterogeneities may also affect transport of bacteria (Fontes et al., 1991; Harvey et al., 1993; Mills et al., 1994; Morley et al.,

1998; Bolster et al., 1999). Studies are needed which examine bacterial transport through intact cores of heterogeneous sediment to enhance our predictive capabilities (Fuller et al., 2000).

Interactions of bacteria with aquifer sediments, groundwater, nutrients and predators result in many transport processes including advection, dispersion, deposition or attachment, entrainment or detachment, growth, die-off and chemotaxis. Mathematical models have been developed that incorporate these processes (e.g., Corapcioglu and Haridas, 1984; Peterson and Ward, 1989) and such models have been successfully used to reproduce experimental data (Peterson and Ward, 1989; Hornberger et al., 1992; McCaulou et al., 1994; Tan et al., 1994; Johnson et al., 1995; Hendry et al., 1999). Bacterial transport has been successfully modeled using the advection–dispersion equation for groundwater solutes with the incorporation of first-order attachment based on colloid–filtration theory (e.g., Harvey and Garabedian, 1991; Hornberger et al., 1992; Martin et al., 1992; Saiers et al., 1994; McCaulou et al., 1994; Bolster et al., 1999; Bolster et al., 2000; Dong et al., 2002). However, it is desirable to model bacterial transport using model parameter values that can be estimated without expensive column or field experiments. To some extent, colloid–filtration theory (Rajagopalan and Tien, 1976; Logan et al., 1995) provides a theoretical basis for estimating the attachment-rate coefficient using bacterial, sediment and fluid properties, but the colloid–filtration theory's applicability to heterogeneous, natural sediments is not clear. In addition, few attempts have been made to quantify other model parameters (e.g., detachment-rate coefficient) based on sediment characteristics. Even bacterial velocity and bacterial-dispersion coefficients are difficult to estimate because these coefficients can differ from those for conservative solutes (Fuller et al., 2000; Dong et al., 2002). It is therefore important to examine and quantify the differences in advection and dispersion among bacteria and conservative solutes.

This study examined the transport of *E. coli* through intact cores of glacial-outwash sediment with the overall goal of enhancing our ability to predict the transport and fate of bacteria in similar geologic environments using easily-measured sediment characteristics. Glacial-outwash aquifer sediments were used due to their heterogeneity and the prevalence of outwash aquifers in North America and Europe (Webb and Anderson, 1996). These aquifers constitute important sources of water in glaciated areas including the north-central region of the USA (Fetter, 2001). There were five main objectives of the experiments: 1) to characterize the transport of *E. coli* and the variability of transport among many cores of intact natural sediments; 2) to compare bacterial transport to conservative solute transport in the same media; 3) to model the transport of *E. coli,* thereby gaining a better understanding of the important processes involved in their transport; 4) to assess how well colloid–filtration theory estimates the attachment-rate coefficient for these intact natural cores and 5) to perform regression analyses, as an alternative to the colloid–filtration theory to explain the variability of bacterial transport behavior in terms of measurable aquifer characteristics. This study focused on assessing the influence of sediment characteristics; therefore, some other factors affecting bacterial transport were kept constant including groundwater chemistry and the type of bacteria used.

2. Experimental methods

2.1. Sediment core acquisition

Aquifer sediments were obtained from a glacial-outwash buried-valley aquifer along the Great Miami River in southwest Ohio. A Versa-sonic K-50® sonic drilling rig (Bowser Morner, Dayton, OH) was used to retrieve 3.05-m long, 10-cm diameter intact sediment cores in polycarbonate liners. Cores were extracted from two sites from depths ranging from 4.8 to 25 m. The cores were

cut into 1-m long sections and transported and stored under saturated conditions at 4 °C. In preparation for the transport experiments, 10-cm long sections were cut from the 3.05-m core for incorporation into a flow-through column assembly. These 10-cm long sections are henceforth referred to as cores.

2.2. Sediment characterization

Sediments used in the study were characterized for physical and biological characteristics. To determine total microbial biomass (MB) and total organic-matter content (OM), sediment samples were taken just above and below the 10-cm cores during cutting. MB was determined by phospholipid phosphate analysis (Findlay et al., 1989; Findlay, 2004). OM was estimated by measuring total organic carbon by weight loss on ignition (Schulte, 1996) and multiplying that mass by a conversion factor of 1.7 (Brady, 1974).

After completion of the transport experiments (described below), hydraulic conductivity (K) of the cores was measured with a constant-head permeameter. Manometers were attached to the top and bottom of the column assembly and water was pumped through at a constant rate until hydraulic-head equilibrium was established. The head differential was measured at three different pumping rates to determine K according to Darcy's law.

The column assemblies were disassembled after the transport experiments and sampled for the distribution of bacteria retained by the sediments (described below). The sediment was weighed wet and dry to determine total porosity and bulk density. The dried sediments were re-saturated with a dispersant (aqueous solution of 5% sodium hexametaphosphate). Grain size distribution was determined using wet-sieving techniques and mesh sizes 25.4, 19.1, 12.5, 6.3, 4.0, 2.83, 2.0, 1.68, 1.0, 0.71, 0.35, 0.177, 0.125 and 0.0625 mm. Grain size determination for sediment <0.0625 mm was performed with a Malver Mastersizer E® at Hamilton College, Clinton, New York. Sediments were characterized in terms of percent gravel (%G), sand (%S), silt (%Si) and clay (%C), median grain size (d_{50}) and the uniformity coefficient, C_u defined as:

$$C_u = d_{60}/d_{10} \tag{1}$$

where d_{60} and d_{10} are the grain sizes for which 60 and 10% by weight of the sediments are finer than those sizes, respectively (Fetter, 2001).

2.3. Transport experiments

Both bromide and bacterial transport experiments were performed on 16 cores (referred to as N1 through N16). The column assembly comprised a headspace purging system to keep the system anaerobic, a peristaltic pump for influent delivery, the sediment core with top and bottom Plexiglas caps and a fraction collector for effluent recovery (Fig. 1). Prior to the setup of a transport experiment, the column apparatus, including all the fittings and tubing, was sterilized with methanol and thoroughly rinsed with distilled water. The column top and bottom caps were then attached to the polycarbonate liner containing the sediments. Two grooves were made along the wall of each cap and O-rings were recessed into the grooves to provide an airtight seal between the column caps and the core section.

Influent groundwater was pumped through the column assembly with a variable-speed, digital Masterflex® L/S peristaltic pump. Water was first pumped into a PVC manifold separating the flow into 20 influent tubes. The 20 tubes were connected to the bottom cap with 20 equally-spaced ports for an equal distribution of flow across the entire core. Effluent left the top of the column assembly through 20 equally-spaced ports in the top cap and was combined in a second

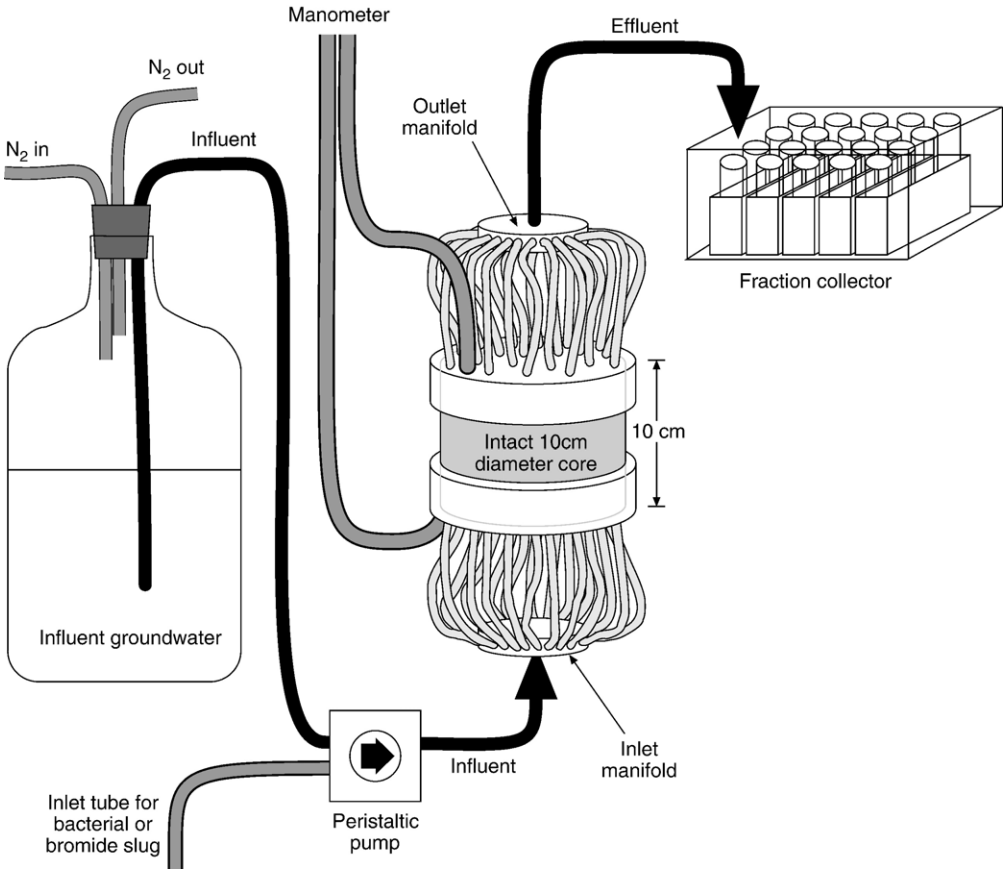

Fig. 1. Schematic diagram of flow-through column assembly.

PVC manifold before flowing to the fraction collector. The entire flow-through apparatus was kept in a refrigerator to maintain a representative aquifer temperature of 12 °C. The ISCO 328 automatic fraction collector contained sterile sample-collection vials and was maintained at 4 °C. To closely mimic the natural aquifer system, transport experiments were performed under anoxic conditions using the headspace purging system in which a low-flow of nitrogen gas was maintained through the air space in the bottle containing the influent groundwater. The influent groundwater used for all experiments was taken from a local aquifer and had low variability with respect to pH (range of 7.26 to 7.37), specific conductance (0.8 mS/cm) and dissolved oxygen content (range of 0.5 to 2.0 mg/L). In the event that any desaturation occurred during the core cutting and column preparation, cores were re-saturated prior to any experiment. Groundwater (free of bromide and *E. coli*) was fed through the core for at least 24 h at a slow flow rate (about 0.2 ml/min) to ensure complete core saturation.

For each core, between one and three bromide transport experiments were conducted before the bacterial breakthrough experiments. For all of the cores except N9 and N16, bromide transport experiments were also conducted after the bacterial experiments. Bromide transport before and after bacterial experiments was compared to determine if running bacterial transport experiments physically altered core flow characteristics. For all breakthrough experiments, a flow rate of about

2 ml/min was used corresponding to an average flow velocity of about 0.16 cm/min or 2.3 m/d. This velocity was chosen to correspond to velocities that are common at the field site from which the cores were taken. For the bromide experiments, immediately following flow of bromide-free groundwater, a 100 mg/L in groundwater bromide solution was introduced into the core as a 10-min, 20-ml pulse followed again immediately with resumption of bromide-free water. Effluent was collected in the fraction collector at 4-min intervals. Bromide experiments were run for 3 pore volumes. Bromide concentrations were measured using a Dionex® DX500 high-performance liquid chromatograph with PeakNet® software.

For bacterial transport experiments, bacteria were also introduced at the core inlet in a 10-min, 20-ml pulse of a bacterial suspension with a mean *E. coli* concentration of 1.9×10^9 colony-forming units (CFU)/ml. Details of the experimental conditions are shown in Table 1. As with bromide experiments, effluent was collected in the fraction collector at 4-min intervals. Bacterial experiments were run for at least 9 pore volumes, typically 13 pore volumes and as many as 32 pore volumes. On six cores, interruption of groundwater flow for 24 h occurred between 11 and 30 pore volumes to detect non-equilibrium, rate-limited transport processes, as indicated by changes in effluent concentration before and after flow interruption (Brusseau et al., 1997).

2.4. Preparation and analysis of bacteria

The bacterial suspension consisted of laboratory-grown *E. coli*. *E. coli* are gram-negative, rod shaped prokaryotes with average cell dimensions of 0.4 by 1 μm. Cells were grown in Luria-bertani broth at 37 °C for 24 h, shaken in a rotary shaker at 100 rpm to an optical density of 0.9 at a wavelength of 610 nm (approximately 2×10^9 CFU/ml). Cells were recovered by centrifugation at 8000 rpm for 20 min at 4 °C and washed twice in 150 ml of groundwater (4 °C). Cells were suspended in groundwater, diluted and plated to determine density. Three subsamples of the suspension were stored with the column assembly at 12 °C to determine time-dependent mortality throughout the length of the experiments (typically <5% over 5 to 7 days).

Table 1
E. coli transport experimental conditions

Core	Flow rate (ml/min)	Input concentration ($\times10^9$ CFU/ml)	Total # samples collected	Total # pore volumes collected	Flow interruption @ (pore volumes)
N1	2.20	1.88	700	30.1	NA[a]
N2	2.09	1.66	650	27.9	25.8
N3	2.07	0.62	687	31.8	29.5
N4	2.06	1.60	350	13.8	11.8
N5	2.03	1.66	350	17.0	14.6
N6	2.03	2.46	350	17.0	14.6
N7	2.10	1.40	300	14.9	NA
N8	2.08	7.10	300	14.3	NA
N9	2.08	1.40	350	13.6	11.7
N10	2.01	2.01	300	10.2	NA
N11	1.98	1.20	300	13.2	NA
N12	2.02	1.08	300	17.1	NA
N13	2.06	1.16	300	11.9	NA
N14	2.10	4.03	200	8.73	NA
N15	2.12	0.96	300	14.1	NA
N16	2.06	0.87	300	14.7	NA

[a] NA is not applicable.

Core effluent was serially diluted in sterile deionized (DI) water to determine *E. coli* abundance. 1 ml of diluted sample was filtered using a 0.47-μm Millipore filter, Gelman membrane filtration apparatus and a vacuum pump. Filters were transferred to pads wetted with 1.5 ml of Lauryl Tryptose broth, placed on lids of a 47-mm mENDO agar plate, and incubated at 37 °C for 2 h. Filters were then transferred from pads to mENDO agar and incubated at 37 °C for an additional 22 h. *E. coli* colonies were enumerated by counting colonies with green metallic sheens. The total number of CFU/ml was determined by multiplying the observed number of colonies by the dilution factor.

The number and distribution of bacteria retained by the cores were determined upon completion of the transport experiments and measurements of *K*. A 5-cm long, 0.56-cm diameter subcore was removed from the center of the top and bottom of each core using a methanol-sterilized syringe. The subcores were aliquoted into 20 0.5-cm subsamples and bacteria suspended by shaking the sediment in 10-ml standard phosphate-buffered saline (PBS) solution. PBS solutions were serially diluted and analyzed for *E. coli* abundance as above. Total abundance was adjusted for time-dependent mortality using the triplicate suspension controls stored with the column assembly.

2.5. Characterization of breakthrough curves

Bromide and bacterial breakthrough curves were generated for each core and were characterized in terms of the normalized maximum concentration (C_{max}/C_0), the time of the arrival of the maximum concentration (T_{peak}), the percentage of input bacteria measured in the effluent during the first 20 h of the experiment (effluent recovery or %ER), and the percentage of input bacteria recovered from the effluent and the core (total bacterial recovery or %TR). The bacterial breakthrough was compared to that of bromide, and the comparison was quantified using the ratio of the bacterial to bromide normalized peak concentration (R_C) and the ratio of the bacterial to bromide peak arrival times in pore volumes (R_T).

2.6. Mathematical and theoretical models

Bromide breakthrough was modeled using a two-region non-equilibrium advection–dispersion model for a nonreactive solute, accounting for rate-limited diffusion between a mobile and an immobile zone (Nkedi-Kizza et al., 1984; Van Genuchten and Wagenet, 1989):

$$\theta_m \frac{\partial c_m}{\partial t} = D_m \theta_m \frac{\partial^2 c_m}{\partial x^2} - v_m \theta_m \frac{\partial c}{\partial x} - \gamma(c_m - c_{im}) \tag{2}$$

$$\theta_{im} \frac{\partial c_{im}}{\partial t} = \gamma(c_m - c_{im}) \tag{3}$$

where θ_m is the mobile volumetric water content (i.e., the proportion of the total volume taken up by the mobile region of the pore space and the effective porosity for bromide) [$L^3\ L^{-3}$], θ_{im} is immobile volumetric water content (i.e., the proportion of the total volume taken up by the immobile region of the pore space) [$L^3\ L^{-3}$], c_m is the concentration of bromide in the mobile region [$M\ L^{-3}$], c_{im} is the concentration of bromide in the immobile region [$M\ L^{-3}$], x is the distance from the core inlet [L], t is time from the initial input of bromide [T], v_m is the pore-water velocity through the mobile region [$L\ T^{-1}$], D_m is the dispersion coefficient in the mobile region [$L^2\ T^{-1}$], and γ is the first-order coefficient of mass-transfer between the mobile and immobile regions [T^{-1}].

Bacterial breakthrough was modeled by incorporating colloid–filtration theory (with bacterial attachment) and a detachment process into a one-dimensional advection–dispersion equation (e.g., Harvey and Garabedian, 1991; Hornberger et al., 1992; Martin et al., 1992; McCaulou et al., 1994; Saiers et al., 1994; Bolster et al., 1999, 2000; Dong et al., 2002):

$$\frac{\partial c}{\partial t} = D\frac{\partial^2 c}{\partial x^2} - v\frac{\partial c}{\partial x} - \frac{\rho_b}{\theta}\frac{\partial s}{\partial t} \tag{4}$$

$$\frac{\rho_b}{\theta}\frac{\partial s}{\partial t} = k_c c - \frac{\rho_b}{\theta}k_y s \tag{5}$$

where c is the concentration of bacteria in the liquid phase [CFU L^{-3}], s is the concentration of bacteria on the solid phase [CFU M^{-1}], v is the interstitial pore-water velocity [$L\ T^{-1}$], D is the dispersion coefficient [$L^2\ T^{-1}$], θ is total porosity [$L^3\ L^{-3}$] and ρ_b is the sediment bulk density [$M\ L^{-3}$], k_c is the first-order deposition or attachment-rate coefficient [T^{-1}], and k_y is the first-order entrainment or detachment-rate coefficient [T^{-1}]. The attachment-rate coefficient can be defined according to colloid–filtration theory (Tien et al., 1979) as:

$$k_c = \frac{3(1-\theta)}{2d_c}\eta\alpha v \tag{6}$$

where d_c is the diameter of the sand grains, α is the sticking efficiency, and η is the single-collector efficiency. According to the model of Rajagopalan and Tien (1976) as modified by Logan et al. (1995), the attachment-rate coefficient is controlled by sediment, bacterial and fluid properties through the single-collector efficiency:

$$\eta = 4A_s^{1/3}N_{Pe}^{-2/3} + A_s N_{Lo}^{1/8} N_R^{15/8} + 0.00338 A_s N_G^{1.2} N_R^{-0.4} \tag{7}$$

where $A_s = 2(1-\gamma^5)/(2-3\gamma+3\gamma^5-2\gamma^6)$, $\gamma = (1-\theta)^{1/3}$, $N_{Pe} = 3\pi\mu d_p d_c q/kT$, $N_{Lo} = 4H/9\pi\mu d_p^2 q$, $N_R = d_p/d_c$, $N_G = g(\rho_p-\rho_f)d_p^2/18\mu q$, d_p is the diameter of the bacteria [L], μ is the fluid viscosity [$M\ L^{-1}\ T^{-1}$], q is the specific discharge [$L\ T^{-1}$], T is temperature [K], k is the Boltzman constant [$M\ L^2\ T^{-2}\ K^{-1}$], H is the Hamaker constant [$M\ L^2\ T^{-2}$], ρ_f is the fluid density [$M\ L^{-3}$], ρ_p is the bacterial density [$M\ L^{-3}$] and g is the gravitational acceleration [$L\ T^{-2}$]. The sticking efficiency can be calculated based on the results of column experiments:

$$\alpha = -\frac{2}{3}\frac{d_c}{(1-\theta)\eta L}\ln(1-R_N) \tag{8}$$

where L is the length of the core [L] and R_N is the fraction of bacterial cell retention in the core (Dong et al., 2002).

2.7. Model calibration and parameter estimation

CXTFIT 2.0 (Toride et al., 1995) was used to fit simulated breakthrough curves of both bromide and bacteria to the observed data and estimate best-fit parameter values. For bromide transport, the average pore-water velocity (through both regions), v, is used as an input parameter and is defined as:

$$v = \frac{Q}{A\theta} \tag{9}$$

where Q is the volumetric flux through the core [$L^3\ T^{-1}$] and A is the cross-sectional area of the core [L^2]; Q, A and θ, all laboratory-measured values. CXTFIT 2.0 solves a dimensionless form of the model described in Eqs. (2) and (3) and estimates β, P and Ω using a nonlinear least square optimization approach based on the Levenberg–Marquardt method. β is the ratio of the mobile region porosity to the total porosity,:

$$\beta = \frac{\theta_m}{\theta} \tag{10}$$

P is the Peclet number defined as:

$$P = \frac{vL}{D} \tag{11}$$

where D is the dispersion coefficient for all the pore space [$L^2\ T^{-1}$]. (CXTFIT actually gives D as an output rather than P). Ω is the dimensionless form of the mass-transfer coefficient:

$$\Omega = \frac{\gamma L}{\theta v} \tag{12}$$

Fitted parameter values allow calculation of the bromide effective porosity through the mobile region, θ_m (based on the fitted β), the bromide dispersivity through the mobile region, α_L (based on the fitted P), and γ (based on Ω).

For bacterial transport, CXTFIT 2.0 solves a dimensionless form of Eqs. (4) and (5), and estimates velocity, the dispersion coefficient and two dimensionless parameters, R and ω where:

$$R = 1 + \frac{k_c}{k_y} \tag{13}$$

and

$$\omega = \frac{k_c L}{v} \tag{14}$$

Fitted parameter values allow calculation of bacterial effective porosity (based on the fitted v), bacterial dispersivity (based on the fitted D and v), and k_c and k_y based on Eqs. (13) and (14). In bacterial transport experiments such as those in this study, the peak concentrations are usually several orders of magnitude higher than the tail concentrations. Because CXTFIT uses equal weights for all observations, the contribution to the objective function from the tail (low-concentrations) is overwhelmed by those from the peak concentrations. CXTFIT will match the peak concentrations well, but not the tail. For this study, the tail was thought to be important as it represents the long-term bacterial-effluent flux after the peak is past. The tail concentration is largely controlled by the detachment-rate coefficient; therefore an accurate tail match provides a good estimate of that parameter. A standard approach to overcome this problem is to weigh the observations by their reciprocal, thereby giving the smaller observations more weight. This was not possible with so many zero concentration values. Alternatively, an accurate tail match can be achieved by artificially extending the tail — adding artificial observations to the end of the tail equal to the average observed tail concentration. We justify this approach with the observation that for all bacterial transport experiments performed, the effluent concentrations quickly leveled off to a relatively constant and persistent tail concentration. For one of the first trial runs, the tail concentration stayed relatively constant for more than 100 pore volumes (over a period of a week). For cores N1, N2 and N3, the tail concentration stayed relatively constant for 28, 30 and 32 pore volumes. Starting with N4, the experiments were run for between 8.7 and 17 pore

volumes (about 20 h), with no indication of diminishing tail concentrations. For all runs, we assumed that the tail persisted beyond the sampling period; based on this assumption, artificial data were added. This method simply provides more weight to the tail for modeling but does not change the fit to the peak of the breakthrough curve. The added artificial points were not used to judge the ultimate fit of the simulation to the observed data, nor are they shown in the figures presented.

Many different initial parameter values were explored during the calibration process. In general, for these simulations, CXTFIT will not run if the initial value parameter values are too far away from the optimized values. Trial-and-error was used to arrive at a set of initial values that resulted in a good calibration. The uniqueness of the final values is supported by the inability of the model to progress using widely-divergent initial values. Different initial values allowing successful model runs led to virtually the same optimized values.

Two other advection–dispersion models were used to fit the observed data. In one of these, a first-order decay term was included to quantify the lumped, net effect of straining, irreversible attachment and natural die-off of bacteria in the aqueous phase during transport. In a separate model, it was assumed that there were two types of attachment/detachment sites: 1) sites for which attachment/detachment was instantaneous so that attached concentrations were in equilibrium with suspended concentrations in groundwater; and 2) sites for which attachment was governed by first-order kinetics (Van Genuchten and Wagenet, 1989). Additional parameter values estimated with these alternative models included the first-order decay rate and the fraction of attachment sites that were at equilibrium.

All three advection–dispersion models were evaluated for the goodness of fit with the model efficiency (*E*),:

$$E = 1 - \frac{\sum_{i=1}^{n} (r_i)^2}{\sum_{i=1}^{n} (c_i - c_{\text{avg}})^2} \tag{15}$$

(Bolster et al., 1999). E was calculated with both the untransformed and the log-transformed observed data and fitted values. While using log-transformed data did not allow inclusion of zero values, it did give greater weight to tail concentrations resulting in an improved indication of model fit. Model selection criterion (MSC) was used to compare the models (Bolster et al., 1999). It measured the information content of each model by accounting for both the goodness of fit and the number of model fitting parameters:

$$\text{MSC} = \ln \frac{\sum_{i=1}^{n} (c_i - c_{\text{avg}})^2}{\sum_{i=1}^{n} (r_i)^2} - \frac{2p}{n} \tag{16}$$

where r_i is the ith residual between model prediction and observation, c_i is the ith observed effluent concentration, c_{avg} is the average of the observed effluent concentrations, n is the number of observations and p is the number of fitting parameters. The best model was the one with the highest goodness of fit obtained with the fewest model parameters, yielding the highest MSC (Bolster et al., 1999). The MSC was also calculated with both untransformed and log-transformed observed and fitted values.

2.8. Investigating the relation of bacterial transport to sediment characteristics

Correlation and multiple linear regression analyses were performed to explore to what degree the measured sediment characteristics account for the variability observed in bacterial transport characteristics and model parameters and to quantify those relationships. Possible regression predictors included K, θ, OM, MB, d_{50}, d_{10}, C_u, %C, %Si, %S and %G. Both untransformed and log-transformed regression models were explored. Forward selection and backward elimination were used to select the best regression models (Chatterjee and Price, 1977). A criterion of a p-value ≤ 0.05 was used to determine whether a predictor should be included in a regression model. The R^2 values presented were adjusted for the number of predictors (R^2-adj). Regression-based predictions were compared to predictions based on colloid–filtration theory.

3. Results

3.1. Sediment characteristics

Generally, the sediments comprised sand and gravel with small amounts of silt and clay, typically less than 10% (Table 2). Great variability existed among the cores in terms of median

Table 2
Physical characteristics of the sediment cores

Core	K[a] (cm/s)	θ[b]	ρ_b[c] (g/cm^3)	d_{50}[d] (mm)	C_u[e]	%Gravel	%Sand	%Silt	%Clay	OM[f] (%)	MB[g] (nm PO_4/g)
N1	1.4E-02	0.26	1.99	1.00	4.27	28.9	67.5	2.97	0.61	0.49	0.45
N2	2.6E-03	0.25	1.97	0.80	3.33	19.6	75.2	4.78	0.38	0.44	0.04
N3	5.6E-03	0.23	2.13	1.62	6.86	44.1	52.4	3.04	0.48	0.38	0.12
N4	6.2E-02	0.27	2.01	2.04	3.22	50.8	46.3	2.66	0.29	0.27	0.06
N5	1.9E-02	0.21	2.15	2.33	9.06	54.4	40.9	4.07	0.67	0.30	0.06
N6	2.2E-02	0.21	2.27	5.33	38.8	80.0	11.0	8.02	1.00	0.31	0.16
N7	6.0E-03	0.22	2.17	2.52	8.00	56.3	39.3	3.77	0.72	0.30	0.65
N8	1.4E-02	0.22	2.10	1.36	7.68	39.2	54.7	5.47	0.67	0.27	0.18
N9	5.3E-04	0.27	2.10	0.50	4.67	18.7	74.2	5.87	1.19	0.52	0.92
N10	1.1E-02	0.30	1.98	1.29	3.66	24.9	71.1	3.15	0.81	0.36	0.20
N11	7.8E-04	0.23	2.19	1.00	9.33	37.0	57.0	4.79	1.22	0.53	0.08
N12	6.8E-03	0.18	2.22	2.90	22.9	57.0	37.3	4.57	1.11	0.38	0.12
N13	4.9E-03	0.26	2.14	1.14	8.21	42.6	52.9	3.86	0.59	0.32	0.57
N14	6.7E-03	0.25	2.12	1.00	6.09	37.3	58.5	3.62	0.59	0.32	0.25
N15	5.0E-03	0.23	2.10	0.98	5.07	29.7	64.7	NA[h]	NA	0.36	0.08
N16	1.5E-02	0.21	2.35	6.25	21.2	69.7	26.5	2.98	0.78	0.18	0.04
Min	5.3E-04	0.18	1.97	0.50	3.22	18.7	11.0	2.66	0.29	0.18	0.04
Max	6.2E-02	0.30	2.35	6.25	38.8	80.0	75.2	8.02	1.22	0.53	0.92
Mean[i]	7.0E-03	0.24	2.13	1.58	7.63	43.1	51.8	4.24	0.74	0.36	0.15

[a] K is hydraulic conductivity.
[b] θ is total porosity.
[c] ρ_b is sediment bulk density.
[d] d_{50} is median grain size.
[e] C_u is the sorting coefficient.
[f] OM is total organic-matter content.
[g] MB is total biomass.
[h] Data are not available.
[i] Geometric means are used for K, C_u, d_{50} and MB; the rest are arithmetic means.

Table 3
Bromide transport calibrated parameter values and uncertainties

Core	Number of runs	D[a] (cm^2/min)			β[b]			ω[c]		
		Value	S.E.[d]	% S.E. of value	Value	S.E.	% S.E. of value	Value	S.E.	% S.E. of value
N1	4	0.068	0.010	15	0.95	0.022	2.3	3.4	0.022	0.64
N2	3	0.070	0.0048	6.8	0.61	0.005	0.80	0.36	0.0044	1.2
N3	4	0.080	0.0090	11	0.66	0.011	1.6	0.51	0.0088	1.7
N4	4	0.022	0.0060	28	0.78	0.009	1.2	0.77	0.0079	1.0
N5	4	0.14	0.0053	3.9	0.41	0.005	1.3	0.39	0.0042	1.1
N6	3	0.35	0.0068	1.9	0.43	0.007	1.5	0.21	0.0045	2.2
N7	4	0.15	0.013	8.6	0.65	0.015	2.2	0.44	0.011	2.4
N8	2	0.098	0.0032	3.3	0.82	0.004	0.49	0.25	0.0033	1.3
N9	1	0.087	0.0059	6.7	0.45	0.006	1.4	0.77	0.0043	0.56
N10	3	0.053	0.0041	7.8	0.73	0.004	0.58	0.27	0.0040	1.5
N11	2	0.13	0.0056	4.4	0.70	0.007	1.0	0.44	0.0048	1.1
N12	3	0.37	0.0094	2.5	0.31	0.009	3.0	0.32	0.0057	1.8
N13	2	0.11	0.0054	5.0	0.50	0.005	1.1	0.36	0.0043	1.2
N14	2	0.061	0.0064	11	0.57	0.006	1.1	0.40	0.0059	1.5
N15	2	0.071	0.0092	13	0.58	0.009	1.6	0.38	0.0084	2.2
N16	1	0.843	0.0042	0.50	0.54	0.004	0.79	0.14	0.0019	1.3
Min	1	0.022	0.0032	0.50	0.31	0.004	0.49	0.14	0.0019	0.56
Max	4	0.84	0.013	28	0.95	0.022	3.0	3.4	0.022	2.4
Mean	2.75	0.17	0.0068	8.1	0.61	0.008	1.4	0.59	0.0065	1.4

[a] D is the dispersion coefficient.
[b] β is the ratio of the mobile region porosity to the total porosity.
[c] ω is the mass-transfer coefficient.
[d] S.E. is the standard error.

grain size, uniformity coefficient, percent gravel and percent sand. (Geometric means are presented when the data appear log-normally distributed.) Based on correlation analysis, sediment characteristics were not related to either the location or the depth from which the core was extracted (data not shown).

3.2. Bromide transport experiments and model simulations

The CXTFIT two-region model (Toride et al., 1995) yielded estimates of bromide transport D, β and Ω (Table 3). Model fits were excellent with R^2 values ranging from 0.982 to 0.9996 and averaging 0.995. Bromide transport before and after the bacterial transport experiments were compared using paired t-tests, and neither the bromide effective porosity or dispersivity values significantly changed.

3.3. Bacterial transport experiments

Core effluent was monitored for *E. coli* prior to their introduction into the cores. *E. coli* were absent from the core effluent prior to their introduction during the transport experiments.

Two of the cores, N9 and N11, exhibited non-classical bacterial breakthroughs with no clear peak or tail and with effluent concentrations that were approximately three orders of magnitude lower than the other cores. The %ERs of these two cores were also more than 2 orders of magnitude lower than those of the other cores (Fig. 2, Table 4).

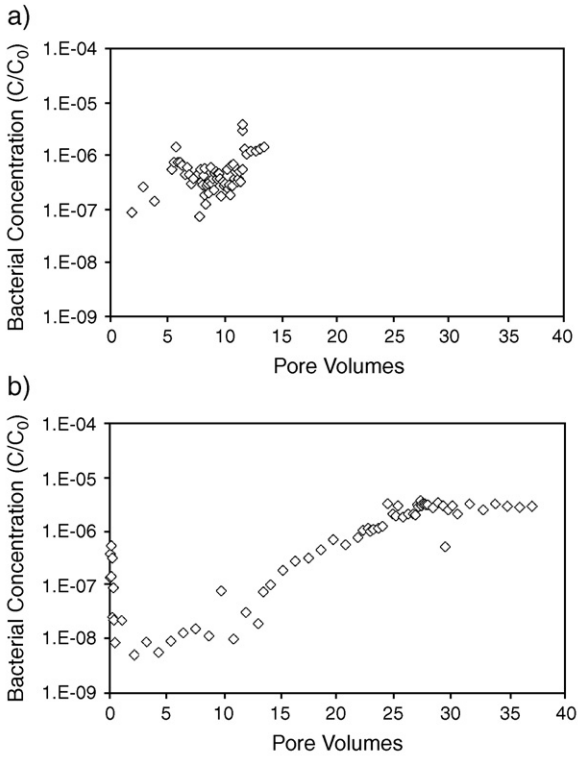

Fig. 2. Atypical *E. coli* breakthrough for columns a) N9 and b) N11.

The patterns in bacterial transport were similar among the other 14 cores, exemplified by core N1 (Fig. 3). A sharp peak concentration appeared shortly after injection (usually within 0.5 pore volumes) and the concentration then dropped rapidly to a relatively constant concentration that continued for the rest of the experiment. The bromide breakthrough through core N1 is shown for comparison (Fig. 3a). For nearly half of the cores, bacterial breakthrough was considerably earlier and the relative effluent peak concentration was much lower than that of bromide (N1, N2, N3, N8, N13, N14 and N15). Some cores had relative effluent peak concentrations of bacteria comparable to those of bromide (N4, N5, N6, N7, N10, N12 and N16); however, the bacterial peak arrival time was still typically earlier. Bacterial breakthrough was compared to that of bromide using R_C and R_T. The average R_C and R_T values were both 0.53 signifying that bacterial peaks were about half the normalized concentration of the bromide peaks but arrived twice as quickly on average. Bacteria arrived more quickly than did bromide, most likely due to pore-size exclusion in which bacteria preferentially move through the largest of the pores with higher permeabilities (Fontes et al., 1991; Dong et al., 2002). Fig. 3b shows the bacterial breakthrough with concentration on a log scale. Note that the normalized effluent concentration fell to between 10^{-5} and 10^{-4} and stayed at that level for the duration of the experiment (30 pore volumes, 15 of which are shown). Again, this pattern was typical for all the cores excluding N9 and N11.

There was great variability in bacterial breakthrough in terms of the maximum concentration and percent effluent recovery (Table 4). An average of about 18% of the bacteria traversed the

Table 4
Summary of *E. coli* transport experiment results

Core	C_{max}/C_0[a]	T_{peak}[b]	R_C[c]	R_T[d]	%ER[e]	%TR[f]
N1	8.46E-03	0.33	5.69E-02	0.41	1.88	98.3
N2	1.45E-03	0.16	8.34E-03	0.30	0.170	108
N3	4.55E-03	0.27	2.71E-02	0.46	0.560	58.8
N4	1.41E-01	0.54	8.64E-01	0.67	30.3	62.4
N5	2.02E-01	0.18	8.18E-01	0.63	34.7	99.9
N6	3.56E-01	0.19	1.47E+00	0.55	59.3	84.8
N7	2.84E-01	0.14	1.72E+00	0.26	32.5	91.0
N8	8.24E-03	0.37	5.76E-02	0.54	1.32	87.1
N9	1.43E-06	NA[g]	1.02E-05	NA	0.00398	98.4
N10	9.95E-02	0.33	7.93E-01	0.52	5.47	101
N11	5.42E-07	NA	4.03E-06	NA	0.000285	88.9
N12	3.05E-01	0.21	8.51E-01	0.97	47.0	85.4
N13	5.09E-03	0.19	2.93E-02	0.46	0.906	92.3
N14	9.16E-03	0.12	4.79E-02	0.23	7.86	102
N15	2.57E-02	0.22	1.30E-01	0.43	4.55	156
N16	2.30E-01	0.23	1.54E+00	1.04	55.8	122

[a] C_{max}/C_0 is the bacterial concentration normalized to the input concentration.
[b] T_{peak} is the arrival time of the maximum concentration in pore volumes.
[c] R_C is the ratio of the bacterial peak concentration to the bromide peak concentration.
[d] R_T is the ratio of the bacterial peak arrival time to the bromide peak arrival time.
[e] %ER is the percent effluent recovery of the bacteria.
[f] %TR is the percent total (effluent and sediment) recovery of the bacteria.
[g] NA is not applicable.

cores in the first 12 pore volumes although small concentrations continued to be found in the effluent no matter how long the experiments were run.

3.4. Flow interruption

Twenty-four hour flow interruptions were included in the transport experiments for six cores (Table 1; Fig. 4). For all six cores, the bacterial-effluent concentration increased after flow resumption with maximum concentration being reached within 1 pore volume after flow resumption. The concentrations increased in all cores by factors between 1.65 and 13.0 (Table 5). Such increases indicate that a kinetic, non-equilibrium process was occurring resulting in an increase in liquid-phase concentrations during static conditions. Flow interruption experiments were also conducted during some of the bromide experiments. There was no indication of a rate-limited process occurring; the bromide concentrations were always the same before and after the flow interruption.

3.5. Bacterial retention by sediments and total bacterial recovery

The %TR ranged between 58.8 and 156%. For three-quarters of the cores, %TR ranged between 84.8 and 102% (Table 4). The overall average %TR of 96% was not significantly different from 100%. The total recoveries indicated there was no significant net bacterial growth or death within the core/groundwater environment that was not accounted for by the time-dependent controls. All the cores retained the most bacteria near the inlet, and bacterial sediment concentrations generally decreased toward the core outlet.

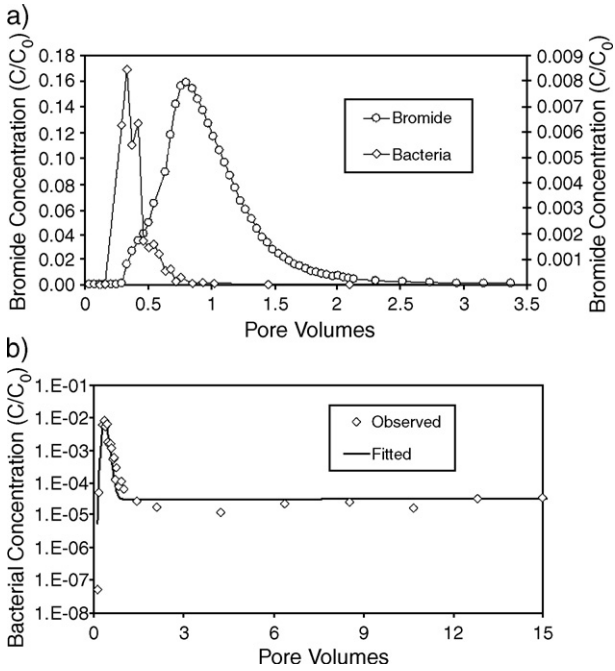

Fig. 3. Typical *E. coli* breakthrough for column N1 shown a) on a linear scale with bromide breakthrough and b) on a log scale with model-fitted curve. Note difference in time scales between the two representations.

3.6. Model simulations of bacterial transport

Measures of E (Eq. (15)) and MSC (Eq. (16)) were applied to the 14 cores with classical bacterial breakthrough curves using both untransformed and log-transformed concentration data. In all but one case, the one-site, non-equilibrium attachment/detachment model resulted in the highest MSC regardless of data transformation. Inclusion of degradation or equilibrium attachment did not significantly improve the model fit. E values for the untransformed data ranged from 0.65 to 1.0 and averaged 0.92 (Table 6). E values for the log-transformed data ranged from 0.18 to 0.97 and averaged 0.79 (Table 6). The low model efficiency of 0.18 for core N13 resulted mostly from the poor match of the first observed concentration, which was anomalously higher than the succeeding measured concentration. When this first concentration was excluded from the analysis, the model efficiency (using log-transformed data) increased to 0.71, and the average model efficiency for all the cores increased to 0.83. An example of a breakthrough curve with a one-site kinetic attachment/detachment model fit is shown for core N1 in Fig. 3b.

Standard errors indicated that model calibration estimated v, D, R and ω reasonably well (Table 7). In only one case (bacterial D for Core N4, Table 7) was the standard error of the parameter estimate greater than 10% of the parameter value. Using calibrated model parameter values, values for effective porosity for bacteria (θ_e), the dispersivity for bacteria (α_L) and k_c and k_y were calculated (Table 8). These parameters exhibited great variability among cores; k_c and k_y appeared log-normally distributed. Bromide-transport estimated parameter values from Table 3 yielded bromide effective porosity and dispersivity values (Table 8). A paired t-test showed that the effective porosity for bacteria was significantly smaller than that for bromide ($p < 0.00005$); however, α_L for bacteria was not significantly different from that of bromide (paired t-test $p > 0.05$).

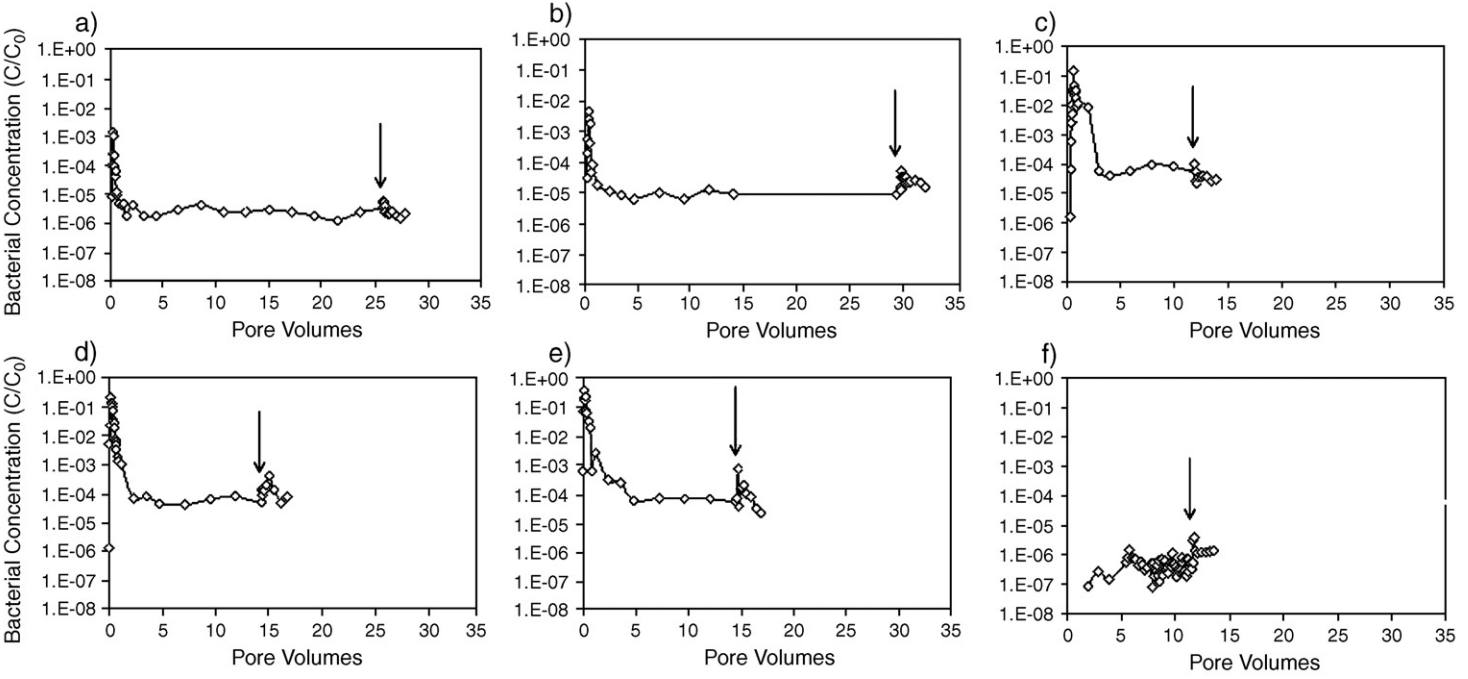

Fig. 4. *E. coli* breakthrough with flow interruption for columns a) N2, b) N3, c) N4, d) N5, e) N6, f) N7. Arrow indicates where the flow was interrupted.

Table 5
Comparison of the bacterial-effluent concentration before and after flow interruption

Core	C/C_0 before[a]	Maximum C/C_0 after[b]	Ratio[c]	Time between before and after samples (pore volumes)
N2	3.61E-06	5.96E-06	1.65	0.0859
N3	9.19E-06	5.04E-05	5.49	0.417
N4	5.69E-05	1.00E-04	1.76	0.0394
N5	4.88E-05	3.80E-04	7.78	0.728
N6	5.37E-05	6.99E-04	13.0	0.194
N9	5.39E-07	3.76E-06	6.97	0.0777

[a] Relative effluent concentration before interruption.
[b] Maximum relative effluent concentration within a pore volume after interruption.
[c] Ratio of the concentration after to the concentration before interruption.

3.7. Bacterial transport in relation to sediment characteristics

Paired correlations among all the measured sediment characteristics, transport characteristics and fitted model parameters are shown in Table 9. Some relationships were stronger when parameters were log-transformed (not shown).

R_T was positively correlated to the median grain size (Table 9), indicating that the smaller the median grain size, the earlier the arrival of the bacterial peak relative to that of bromide; conversely, larger grain sizes were associated with less differential advection (i.e., less pore-size exclusion). R_T was also weakly correlated to the uniformity coefficient (Table 9) indicating well-sorted sediment showed greater differential advection. This correlation, however, may be an artifact of the high degree of correlation between median grain size and the uniformity coefficient ($r=0.83$). The best regression model for R_T, (Table 10, equation i) indicated that the sediment property that accounted for, and subsequently predicted, the variation in differential advection was median grain size.

Later peak bacterial breakthroughs, more similar to bromide breakthroughs, were associated with greater peak concentrations. The ratio of the bacterial peak concentration to the bromide

Table 6
E. coli transport modeling goodness of fit

Core	Model efficiency with untransformed data	Model efficiency with log-transformed data
N1	1.00	0.89
N2	1.00	0.74
N3	1.00	0.93
N4	0.81	0.71
N5	0.92	0.96
N6	0.90	0.96
N7	0.65	0.71
N8	1.00	0.88
N10	1.00	0.42
N12	0.98	0.91
N13	0.65	0.18
N14	1.00	0.97
N15	0.97	0.90
N16	0.96	0.97
Min	0.65	0.18
Max	1.00	0.97
Mean	0.92	0.79

peak concentration (R_C) was, like R_T, also correlated to the median grain size. The best regression model (Table 10, equation ii) included median grain size and total microbial biomass. Core N7 was removed as a statistical outlier (Chatterjee and Price, 1977) as the R_C for N7 was outside the equation's 99.5% prediction interval.

Colloid–filtration theory predicts that bacterial abundance in core effluent will be positively correlated to the grain size of the transport medium. We found strong linear relationships between median grain size and both %ER and C_{max}/C_0 (both of which reflect effluent bacterial abundance) (Table 10, equation iii and Fig. 5a and Table 10, equation iv and Fig. 5b, respectively).

The peak bacterial concentration arrived more quickly (i.e., lower T_{peak}) when the transport media had lower hydraulic conductivities (K) and were more poorly-sorted (higher C_u) as shown in the best regression model for T_{peak} (Table 10, equation v).

The relationships among model parameters θ_e, α_L, k_c and k_y and sediment characteristics were also investigated using multiple linear regression. Two similar regression models were found relating effective porosity for bacteria and sediment characteristics: one using K and C_u and one using K and percent sand content (Table 10, equations vi and vii, respectively). For these cores, the percent sand content was negatively correlated to the C_u (the more well-sorted the sediment, the more sand it contained).

Previous work suggests dispersivity increases with increasing sediment heterogeneity (Fetter, 1999). A regression model was found relating dispersivity to C_u (Table 10, equation viii, Fig. 6a) For these cores, d_{50} was, highly correlated to C_u (Table 9), and d_{50} yielded a slightly stronger regression model (Table 10, equation ix, Fig. 6b).

Table 7
E. coli transport calibrated parameter values and uncertainties

Core	v[a] (cm/min)			D[b] (cm^2/min)			R[c]			ω[d]		
	Value	S.E.[e]	% S.E. of value	Value	S.E.	% S.E. of value	Value	S.E.	% S.E. of value	Value	S.E.	% S.E. of value
N1	0.23	9.5E-04	0.41	0.14	9.9E-04	0.71	3.1E+03	2.6E-04	8.49E-06	5.2	1.0E-03	0.019
N2	0.79	3.5E-05	0.0044	0.022	4.8E-05	0.22	1.8E+04	2.7E-05	1.51E-07	6.8	4.6E-05	6.7E-04
N3	0.30	1.4E-03	0.46	0.14	1.7E-03	1.2	6.4E+03	3.4E-04	5.27E-06	6.5	1.6E-03	0.025
N4	0.14	1.1E-02	7.5	0.10	1.1E-02	11	1.2E+03	5.4E-03	4.67E-04	1.8	6.0E-03	0.34
N5	0.36	9.4E-03	2.6	0.80	9.4E-03	1.2	2.4E+03	4.9E-03	2.05E-04	1.4	4.9E-03	0.36
N6	0.41	6.9E-03	1.7	0.82	7.3E-03	0.88	1.4E+02	4.2E-03	2.95E-03	0.18	4.7E-03	2.5
N7	0.92	2.5E-02	2.7	2.3	2.4E-02	1.1	6.0E+04	6.2E-03	1.02E-05	2.7	3.1E-02	1.2
N8	0.26	6.9E-04	0.26	0.10	7.6E-04	0.73	1.1E+04	2.4E-04	2.12E-06	5.3	5.6E-04	0.011
N10	0.26	1.5E-03	0.58	0.030	1.5E-03	5.1	2.9E+03	8.2E-04	2.82E-05	4.1	8.2E-04	0.020
N12	0.60	3.1E-02	5.3	2.0	3.1E-02	1.5	1.2E+03	1.7E-02	1.36E-03	0.92	1.6E-02	1.7
N13	0.49	1.5E-03	0.31	0.15	2.0E-03	1.3	2.0E+03	3.6E-04	1.81E-05	6.6	1.9E-03	0.028
N14	0.77	1.5E-04	0.020	0.10	1.8E-03	1.9	6.7E+04	8.6E-06	1.28E-08	3.7	1.7E-03	0.046
N15	0.37	1.4E-03	0.37	0.34	1.5E-03	0.44	5.6E+03	3.7E-04	6.73E-06	4.3	1.5E-03	0.034
N16	0.34	9.2E-03	2.7	1.7	9.1E-03	0.53	8.0E+02	4.3E-03	5.33E-04	0.89	4.4E-03	0.50
Min	0.14	3.5E-05	0.0044	0.022	4.8E-05	0.22	1.4E+02	8.6E-06	1.3E-08	0.18	4.6E-05	6.7E-04
Max	0.92	3.1E-02	7.5	2.3	3.1E-02	11	6.7E+04	0.017	3.0E-03	6.8	3.1E-02	2.5
Mean	0.45	7.2E-03	1.8	0.62	7.3E-03	2.0	1.3E+04	0.0032	4.0E-04	3.6	5.5E-03	0.49

[a] v is velocity.
[b] D is the dispersion coefficient.
[c] R is the retardation factor.
[d] ω is the mass-transfer coefficient.
[e] S.E. is the standard error.

Table 8
E. coli and bromide transport modeling results

Core	k_c^a (min^{-1})	k_y^b (min^{-1})	*E. coli* transport θ_e^c	Bromide transport θ_m^d	*E. coli* transport α_L^e (cm)	Bromide transport α_L (cm)
N1	1.2E-01	3.9E-05	0.12	0.25	0.60	0.59
N2	5.4E-01	3.0E-05	0.034	0.15	0.028	0.65
N3	2.0E-01	3.1E-05	0.087	0.15	0.45	0.56
N4	2.6E-02	2.2E-05	0.18	0.21	0.69	0.19
N5	4.9E-02	2.1E-05	0.071	0.087	2.2	1.1
N6	7.7E-03	5.4E-05	0.062	0.093	2.0	2.4
N7	2.4E-01	4.1E-06	0.029	0.15	2.5	1.1
N8	1.4E-01	1.2E-05	0.10	0.18	0.40	0.83
N10	1.1E-01	3.7E-05	0.098	0.22	0.11	0.65
N12	5.5E-02	4.5E-05	0.043	0.054	3.3	2.4
N13	3.2E-01	1.6E-04	0.053	0.13	0.30	1.1
N14	2.8E-01	4.2E-06	0.035	0.14	0.12	0.56
N15	1.6E-01	2.9E-05	0.072	0.13	0.92	0.58
N16	3.1E-02	3.8E-05	0.076	0.12	5.0	7.0
Min	7.7E-03	4.1E-06	0.029	0.054	0.028	0.19
Max	5.4E-01	1.6E-04	0.18	0.25	5.0	7.0
Average[f]	1.0E-01	2.6E-05	0.076	0.15	1.3	1.4

[a] k_c is the attachment-rate coefficient.
[b] k_y is the detachment-rate coefficient.
[c] θ_e is the effective porosity for bacteria.
[d] θ_m is the mobile region effective porosity for bromide.
[e] α_L is dispersivity.
[f] Geometric means are used for k_c and k_y; the rest are arithmetic means.

As predicted by colloid–filtration theory, the attachment-rate coefficient was negatively correlated with log-transformed d_{50} (Table 9; Table 10, equation x; Fig. 7). Interestingly, we found an alternate and stronger regression model for k_c not predicted by colloid–filtration theory, using K and C_u (Table 10, equation xi). Core N6 was excluded as an influential point, but results were very similar with or without N6.

In exploring regression models for the detachment-rate coefficient, no strong relationships were found using all 14 cores. One core, N13, has an associated k_y-value that was between 3 and 40 times the other calibrated values (Table 8). With N13 removed from the regression analysis as a statistical outlier, the detachment-rate coefficient was positively-correlated to median grain size, the organic-matter content and the log-transformed effective porosity (Table 10, equation xii). The k_y-value of N13 was outside the 99.9% prediction interval for the regression equation. Alternatively, using the log-transformed values of k_y yielded a regression model, which included log θ_e, C_u and log K (Table 10, equation xiii). The log k_y-value of N13 was again outside the 99% prediction interval for this regression model.

3.8. Application of colloid–filtration theory and comparison to regression approach

The attachment-rate coefficient regression equation, shown in Table 10, equation xi, accounted for 89% of the observed variability in empirically-derived coefficients (i.e., CXTFIT-calibrated values) from the 14 column experiments. We propose this approach as an alternative to colloid–filtration theory, which estimates the attachment-rate coefficient based

Table 9
Correlation matrix of sediment characteristics and fitted parameters (rounded to two digits)

	K	θ	ρ_b	d_{50}	d_{10}	C_u	%G	%S	%Si	%C	%OM	MB	k_c	k_y	*E. coli* θ_e	Br θ_m	*E. coli* α_L	Br α_L	R_c
θ	0.13																		
ρ_b	−0.14	**−0.74**																	
d_{50}	0.28	*−0.56*	**0.77**																
d_{10}	**0.74**	0.33	−0.32	0.02															
C_u	0.06	**−0.64**	**0.77**	**0.83**	−0.37														
%G	0.37	**−0.66**	**0.78**	**0.89**	0.05	**0.81**													
%S	−0.34	**0.68**	**−0.80**	**−0.89**	0.02	**−0.85**	**−1.00**												
%Si	−0.20	−0.32	0.30	0.19	**−0.64**	*0.60*	0.20	−0.28											
%C	−0.44	−0.29	0.50	0.17	**−0.71**	0.46	0.11	−0.16	*0.54*										
%OM	−0.46	0.29	−0.40	**−0.63**	*−0.54*	−0.31	**−0.66**	**0.62**	0.18	0.39									
MB	−0.04	*0.57*	−0.37	−0.13	0.14	−0.19	−0.29	0.30	−0.21	0.08	0.02								
k_c	−0.53	0.29	−0.42	*−0.57*	−0.18	−0.48	*−0.61*	*0.60*	−0.06	−0.48	0.41	−0.09							
k_y	−0.15	0.16	0.13	0.00	0.02	0.17	0.06	−0.06	0.08	0.09	0.05	0.01	0.15						
E. coli θ_e	**0.80**	0.42	−0.38	−0.07	**0.78**	−0.26	−0.07	0.10	−0.35	−0.39	−0.08	0.15	−0.51	−0.11					
Br θ_m	0.29	**0.79**	**−0.73**	−0.46	0.51	*−0.63*	*−0.57*	*0.59*	−0.47	−0.53	0.29	0.40	0.09	−0.16	*0.64*				
E .coli α_L	0.02	**−0.70**	**0.82**	**0.85**	−0.15	*0.62*	**0.75**	**−0.74**	0.06	*0.57*	−0.52	−0.24	−0.51	−0.08	−0.21	*−0.56*			
Br α_L	−0.05	−0.48	**0.79**	**0.86**	−0.05	*0.61*	*0.62*	*−0.61*	0.06	0.46	*−0.56*	−0.13	−0.36	0.10	−0.17	−0.41	**0.86**		
R_c	0.36	−0.38	*0.52*	**0.82**	0.08	*0.59*	**0.78**	**−0.77**	0.05	0.12	*−0.60*	0.11	−0.53	−0.17	−0.07	−0.29	**0.76**	*0.57*	
R_T	0.30	−0.46	*0.55*	**0.66**	0.25	0.50	*0.55*	−0.53	−0.04	0.46	−0.45	−0.03	**−0.66**	0.11	0.24	−0.38	**0.74**	**0.72**	0.43

Correlation coefficients with $0.05 \geq p$-values > 0.01 are in italics. Correlation coefficients with p-values ≤ 0.01 are in bold. Fitted parameter values do not include cores N9 and N11.

Table 10
Regression analysis results

Equation reference number	Equation	R^2-adjusted (%)	Regressor p-values	Overall p-values	Degrees of freedom
i	$R_T=0.39+0.59\ \log(d_{50})$	43	0.007	0.007	12
ii	$R_C=-0.20+0.31\ d_{50}+0.30$ MB	86	<0.001 0.029	<0.001	10
iii	$\%ER=1.4+75\ \log(d_{50})$	87	<0.001	<0.001	12
iv	$C_{max}/C_0=0.018+0.41\ \log(d_{50})$	74	<0.001	<0.001	12
v	$T_{peak}=0.87+0.24\ \log(K)-0.16\ \log(C_u)$	63	0.001 0.017	0.002	11
vi	$\log\ \theta_e=0.044+0.50\ \log\ K-0.25\ \log\ C_u$	58	0.001 0.076	0.003	11
vii	$\log\ \theta_e=-0.26+0.61\ \log\ K+0.0062\ \%S$	66	<0.001 0.021	0.001	11
viii	$\log\ \alpha_L=-1.41+1.3\ \log\ C_u$	44	0.006	0.006	12
ix	$\log\ \alpha_L=-0.66+1.9\ \log\ d_{50}$	61	0.001	0.001	12
x	$\log\ k_c=-0.64-1.5\ \log\ d_{50}$	61	0.001	0.001	12
xi	$\log\ k_c=-2.6-0.97\ \log\ K-0.030\ C_u$	89	<0.001 0.001	<0.001	11
xii	$k_y\times10^5=-2.6+0.94\ d_{50}+18$ OM$+2.4\ \log\ \theta_e$	76	<0.001 0.001 0.028	<0.001	9
xiii	$\log\ k_y=-4.5+1.8\ \log\ \theta_e+0.027\ C_u-0.89\ \log\ K$	57	0.004 0.006 0.024	0.013	9

on fluid, sediment and bacterial properties (Eqs. (6), (7) and (8)). Using Eqs. (6) and (7) (colloid–filtration theory) and several assumptions outlined below, k_c values were calculated for each of the 14 cores. Values for porosity and median grain size were taken from laboratory measurements (Table 2). The specific discharge was experimentally derived based on the flow rate and cross-sectional core area. The bacterial cells used for the column experiments were rod shaped with a length of 1.2 μm and a width of 0.39 μm yielding a surface area of approximately 0.93 μm^2. A cell diameter of 0.54 μm was used in Eq. (7) representing a sphere of the same approximate surface area. A bacterial density of 1080 kg/m^3 was assumed (Bolster et al., 1999). The temperature was 12 °C, and the fluid density (999 kg/m^3) and fluid viscosity (1.24×10^{-3} Pa s) were calculated based on this temperature. Pore-water velocity was the best-fit value obtained from the CXTFIT model calibration of bacterial transport (Table 8). Still unknown for this calculation was the sticking coefficient, α. We first assumed $\alpha=1$ (all collisions with the collector surface result in attachment; Hornberger et al., 1992; Saiers et al., 1994). The resulting k_c values were strongly correlated to the empirically-derived values (Fig. 8). To reduce leverage of the highest k_c value and heteroscedasticity inherent in the relationship, regression analysis was conducted using weighted least squares (Chatterjee and Price, 1977). The weights used were inversely proportional to the values derived using colloid–filtration theory. The resulting regression equation had a slope of 0.77 (R^2-adj=0.72, $p<0.001$), indicating that colloid–filtration theory was able to account for 72% of the variability observed in the CXTFIT-calibrated k_c values and tended to overestimate the k_c values. The slope, however, was not significantly different from 1.0 ($p>0.05$).

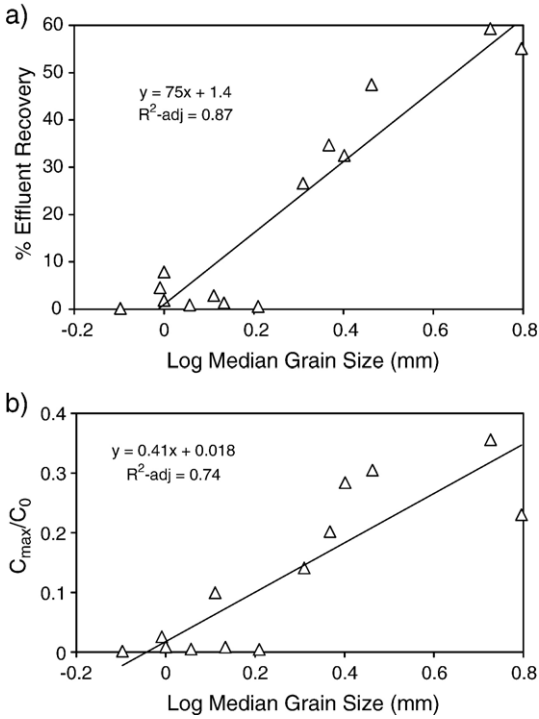

Fig. 5. Relation of breakthrough-curve characteristics (a) percent effluent recovery and (b) C_{max}/C_0 to median grain size.

Alternatively, it is possible to calculate values for the sticking coefficient based on the retention of bacteria within the sediment core according to Eq. (8) (Dong et al., 2002). The fraction of bacteria retained (R_N) in each core was:

$$R_N = 1 - \frac{\%ER}{100} \tag{17}$$

where the %ER is the percent effluent recovery presented in Table 4. When the retention data were taken into account, there was a much stronger agreement (R^2-adj = 0.92, $p < 0.001$) between the values calculated by the colloid–filtration theory and the CXTFIT-calibrated values (Fig. 9). In this case, colloid–filtration theory under predicted the CXTFIT-calibrated values. The slope for this relationship was 1.1, but was not significantly different from 1.0. The strong correlation indicated that colloid–filtration theory with retention data accounted for nearly all of the variability observed in the CXTFIT-calibrated values, as did the much simpler best-fit regression model.

In the above estimates, however, key parameter values required to apply colloid–filtration theory were derived from the bacterial transport experiments. Results shown in Fig. 9 were dependent on the bacterial retention data from the column experiments, and results shown in Figs. 8 and 9 used the pore-water velocities derived from modeling bacterial breakthroughs with CXTFIT. Given fitted bacterial breakthroughs curves, there is no need to apply colloid–filtration theory. How reliable would estimates based on colloid–filtration theory be in the absence of bacterial-breakthrough experiments? To answer this question, k_c values were recalculated using pore-water velocity estimates derived from bromide transport experiments and without the

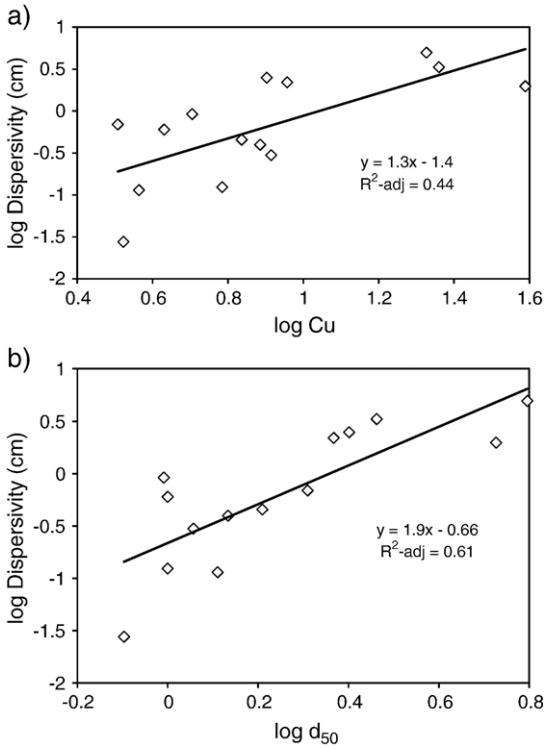

Fig. 6. Relation of CXTFIT-calibrated dispersivity values to (a) the uniformity coefficient and (b) the median grain size.

benefit of the retention data. Without the retention data, α was again set to 1. As shown in Fig. 10, these values did not agree as well with the CXTFIT-calibrated k_c values. Regression analysis indicated that only 28% of the observed variability in CXTFIT-calibrated values was accounted for by colloid–filtration theory applied without the benefit of bacterial transport experiments. The

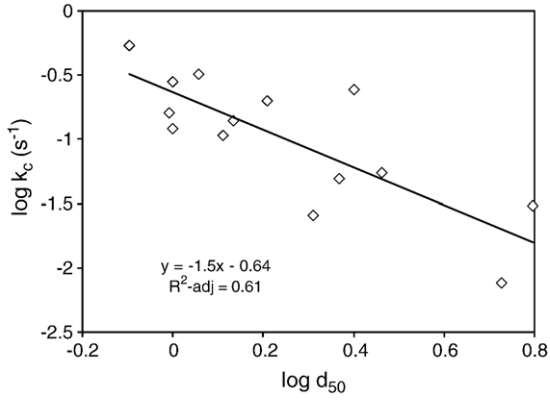

Fig. 7. Relation of CXTFIT-calibrated attachment-rate coefficient values to the median grain size.

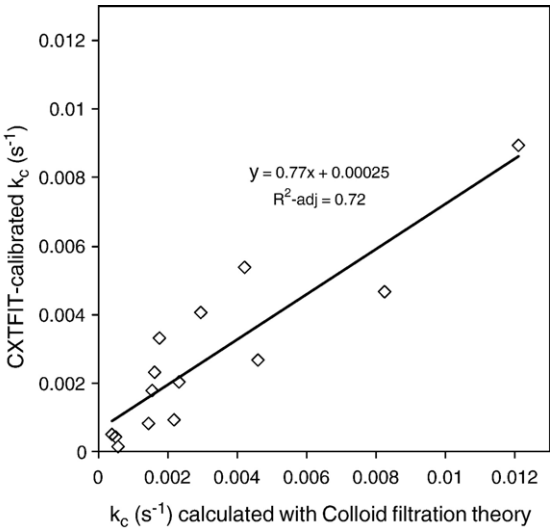

Fig. 8. Comparison of CXTFIT-calibrated attachment-rate coefficient values and those derived from the colloid filtration theory assuming that $\alpha = 1$. Pore-water velocities are based on bacterial breakthroughs.

intercept from this relationship was not significantly different from 0, so the regression was re-run setting the intercept equal to 0 and using weighted least squares to reduce the heteroscedasticity (Chatterjee and Price, 1977) with weights inversely proportional to colloid–filtration theory values. The new relationship had a slope of 1.97, significantly different from 1 ($p < 0.05$). Colloid–filtration theory applied in this way substantially under predicted the attachment-rate coefficient. The analyses presented here indicated that, in lieu of running bacterial transport experiments, the regression approach (Table 10, equation xi) accounts for a much greater proportion of the variability in the observed CXTFIT-calibrated k_c values than did colloid–filtration theory.

The 14 k_c-values estimated with colloid–filtration theory without the benefit of the bacterial transport experiments (Fig. 10) were used in forward CXTFIT simulations to determine agreement between the observed and predicted breakthrough curves. Estimates of velocity and dispersivity were based on the bromide-experimental results. Forward simulations were also performed using parameter values estimated with the regression approach and the CXTFIT-calibrated parameter values. The regression approach uses equations vii, ix, xi and xii from Table 10 to estimate the bacterial effective porosity, dispersivity, attachment-rate coefficient and detachment-rate coefficient, respectively. The regression and colloid–filtration theory approaches cannot be formally compared because the forward simulations are conducted on the same cores for which the regression equations were derived; i.e., a comparison gives no indication of how well the approaches would compare on a different set of cores. A true test on a different set of cores is beyond the scope of this paper. Nonetheless, the forward simulations using the regression-based simulations are informative as they reflect the goodness of fit of the regression equations. The breakthrough curves were reproduced most accurately, of course, using the CXTFIT-calibrated values; those values were also used in the forward simulations as a benchmark for comparison.

Based on forward CXTFIT simulations on the 14 cores, the geometric mean ratios of the predicted C_{max} to the observed C_{max} were 0.80, 0.50 and 0.31 for the CXTFIT, regression and colloid–filtration theory approaches, respectively. The respective geometric mean ratios of the

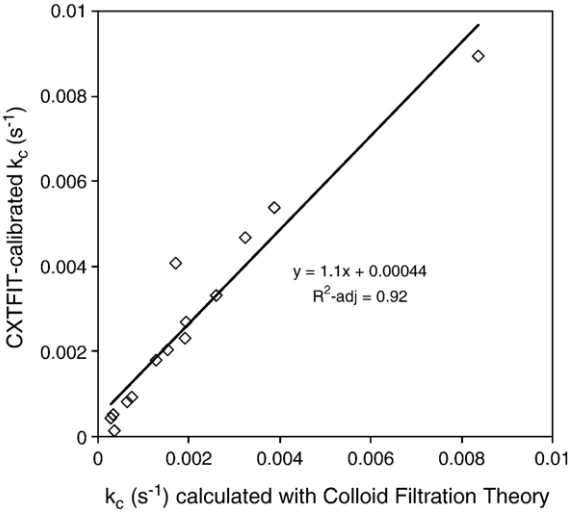

Fig. 9. Comparison of CXTFIT-calibrated attachment-rate coefficient values and those derived from colloid-filtration theory. Values for α are from retention data. Pore-water velocities are based on bacterial breakthroughs.

predicted to the observed C_{max} arrival times were 1.1, 1.2 and 1.7. On average, all methods under predicted the maximum concentration and over predicted the peak arrival time. In addition, colloid–filtration theory does not include a detachment-rate coefficient, so no tail was simulated. The different approaches worked better for some cores than for others. An example set of simulations in which colloid–filtration theory substantially under predicted the maximum

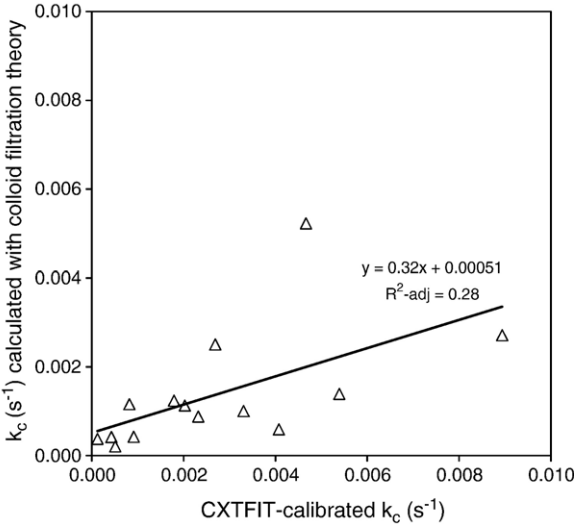

Fig. 10. Comparison of CXTFIT-calibrated attachment-rate coefficient values and those derived from the colloid filtration theory assuming that $\alpha = 1$. Pore-water velocities are based on bromide breakthroughs.

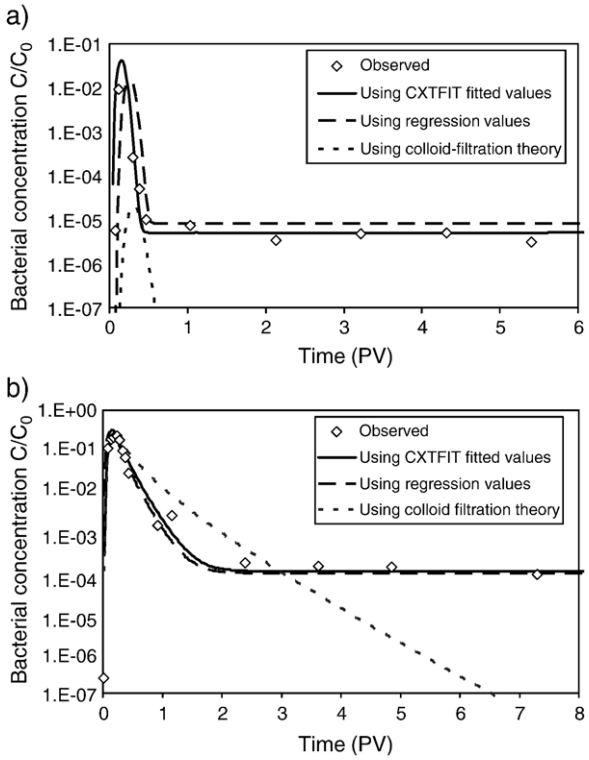

Fig. 11. Direct simulations of bacterial transport using different methods of parameter-value estimation: CXTFIT-calibrated values, regression models and the colloid–filtration theory. Simulations shown for columns a) N14 and b) N16.

concentration is shown in Fig. 11a for core N14. Fig. 11b shows the simulations for core N16, an example where the colloid–filtration theory performed well until the tail was reached.

4. Discussion

4.1. Use of intact, natural cores

Only a few investigations have studied bacterial transport using cores of intact, natural sediments (Smith et al., 1985; Bolster et al., 1999; Fuller et al., 2000; Dong et al., 2002). Such studies are important as repacked cores may not replicate the structure and preferential flow pathways inherent in natural sediments (Dong et al., 2002). Most of the previous column studies with intact, natural cores used aquifer sediments consisting of relatively homogeneous sands (Oyster, Virginia: Bolster et al., 1999; Fuller et al., 2000; Dong et al., 2002). These studies are either limited in the number of cores studied and/or the range of key sediment characteristics (Dong et al. (2002), four cores, d_{50} 0.210–0.293 mm; Fuller et al. (2000), three cores, d_{50} 0.174–0.280 mm; Bolster et al. (1999), C_u 1–5). In contrast, this study examined bacterial transport through 16 intact cores from a glacial-outwash aquifer that were much more heterogeneous (d_{50} 0.50–6.3 mm, C_u 3.2–39) than those from the Oyster, VA site. The greater variability in sediments led to great variability in bacterial transport. The use of 16 highly-variable cores

allowed the identification of d_{50}, MB, K, C_u, OM, %S and θ_e as potential controlling factors and the development of regression models that quantify the relationships.

4.2. Sources of error and total recovery

One possible source of error in interpreting the results in general was the fact that CO_2 was not used to pre-saturate the cores, prior to water saturation. It is possible that air bubbles were trapped within the cores and served as attachment sites for bacteria. There was no evidence of this, as no gas bubbles were observed within the cores.

Some of the %TR values were problematic. Ideally, the %TR should be 100%. While the average for the 16 cores was 96%, the range was great (58.8 to 156%). The method used to extract sediment samples from within each core sampled only a small portion of the total volume of sediments (a 0.56-cm diameter subcore taken from a 10-cm diameter full core). Bolster et al. (1999) demonstrated that deposited bacterial concentrations can vary greatly across any transverse cross section of a core; therefore, the total recoveries, which included bacteria retained by the sediment, should be interpreted as rough estimates.

4.3. Bacterial transport characterization and comparison to conservative-tracer transport

In this study, bacterial breakthrough curves were characterized by a sharp peak and a long tail of a relatively constant concentration. Similar breakthrough curves have been previously observed (Fontes et al., 1991; Harvey et al., 1991; Scholl et al., 1991; Hendry et al., 1999). These curves indicate that bacterial transport is influenced by non-equilibrium attachment/detachment. Flow interruption experiments, applied to six cores, confirmed that attachment/detachment was a non-equilibrium process. The rate coefficient is, perhaps, the most crucial parameter to determine as it ultimately controls the estimated peak-effluent concentration. The detachment-rate coefficient is also important as detachment is a potential source of continuing contamination, long after a peak passes through a given location (Bolster et al., 2000). Gerba and Bitton (1984) noted that substantial numbers of bacteria transport in groundwater over great distances. Bolster et al. (1999) hypothesized that a small fraction of the bacterial population with much lower sticking efficiencies explained such observations; however, first-order rate-limited detachment, as observed in this study, can also explain this behavior.

Early breakthrough of bacteria with respect to bromide was observed on all but one core. Such early breakthrough is probably due to pore-size exclusion where, due to their larger size, bacteria move through only a subset of the pore space available for bromide transport leading to an effective porosity for bacterial transport that is significantly smaller than that for bromide transport. Pore-size exclusion and the resulting differential advection (with average flow velocity for bacterial transport faster than that for bromide transport) was also noted in column experiments by Dong et al. (2002) and by Fontes et al. (1991). We found that the degree of differential advection was inversely correlated to median grain size and therefore positively correlated to k_c. This finding is in agreement with Dong et al. (2002) who found a positive correlation between the degree of differential advection and the abundance of clays and grain coatings of metal hydroxides and an inverse correlation between the abundance of coatings and grain size. One explanation is that an increasing k_c results in a smaller and thinner peak, with the peak concentration arriving sooner. Conservative-tracer experiments are commonly used to determine the physical transport parameter values for bacterial transport simulations (e.g., Harvey et al., 1991; Tan et al., 1994; McCaulou et al., 1995; Morley et al., 1998; Hendry et al., 1999;

Fuller et al., 2000). Our results indicate that this approach is valid for estimating dispersivity, but not for estimating bacterial velocity or effective porosity. In addition, when calculating k_c using colloid–filtration theory, bacterial-transport-based estimates of pore-water velocity proved superior to bromide transport based estimates. This confirms the previous finding of Dong et al. (2002) and expands this generalization to a wider range of sediment types.

4.4. Modeling bacterial transport and implications for bacterial processes

A simple transport model incorporating first-order attachment/detachment, advection and dispersion was able to adequately reproduce 14 out of 16 bacterial breakthrough curves including the early peak breakthrough and the very long tail with little change even after 30 pore volumes. Other more complex models did not substantially improve model fits (data not shown). For the core lengths and time scales applied here, first-order attachment/detachment was the only important controlling process for bacterial transport other than advection and dispersion. The roles of such other processes as straining, irreversible attachment, equilibrium attachment/detachment, chemotaxis, growth, predation and natural die-off were minimal. Dong et al. (2002) also successfully applied the same transport model. Hendry et al. (1999) had similar results for the bacterium G4PR1; however, for the bacterium *Klebsiella oxytoca*, it was necessary to include irreversible sorption; the reason for the difference between the two bacterial strains was unknown. Harvey et al. (1991) indicated if they assumed reversible attachment was fast (equilibrium conditions) the model required irreversible sorption; however, if they assumed kinetic reversible attachment, no irreversible sorption was necessary.

Calculation of bacterial straining factors, based on the method by Matthess and Pekdeger (1985) indicated that straining was not a significant process for the bacterial experiments involved in this study. Bradford et al. (2003), however, suggested that the method by Matthess and Pekdeger (1985) may underestimate straining. Based on results from their column experiments, Bradford et al. (2003) suggest an alternative equation to predict the influence of straining:

$$k_{str} = 269.7\left(\frac{d_p}{d_{50}}\right)^{1.42} \qquad r^2 = 0.93 \tag{18}$$

where k_{str} is the straining coefficient. While Bradford et al. (2003) did not state the minimum values for k_{str} below which straining can be ignored, it is possible to assess the importance of straining by comparing this study to the Bradford et al. (2003) study. Bradford et al. (2003) compared models that included straining along with linear reversible attachment/detachment to models that did not include straining. The values Bradford et al. (2003) derived for k_{str} were, on average, three times greater than their values derived for k_c, not including straining; the ratios of k_{str} to k_c, ranged from 0.68 to 27. When both reversible attachment and straining were included in the model, values for k_{str} were on average six times greater than k_c, and ratios of k_{str} to k_c, ranged from 2.1 to 20. Applying Eq. (18) to our results yielded ratios of k_{str} to k_c that ranged from 0.0069 to 0.088 and averaged 0.022. These results indicated that straining was less important (by a factor of >100) for natural, poorly-sorted sediments used in this study compared to sieved-sand, laboratory-packed cores used by Bradford et al. (2003).

Bacterial transport through two cores, N9 and N11, could not be modeled. Breakthrough curves for these cores were similar to some shown by Fuller et al. (2000). It is not known why these cores differed from the other 14 cores. While all sediments used in this study were largely sand and gravel with very small silt and clay contents, cores N9 and N11 had the highest clay (1.19 and 1.22%) and organic-matter contents. While these clay contents are not considered high

(and only slightly higher than in cores N6 and N12), if the clay was concentrated as a layer across the core, it could have acted as an effective barrier. Such thin layers may not be detectable by bulk grain size analysis. Alternatively, there may be clay and/or organic-matter content beyond which early breakthrough peaks do not occur. Clearly more research is needed to identify under what conditions the nature of bacterial transport changes so dramatically.

4.5. Implications of the multiple regression analyses

Empirical equations were developed using multiple regression analyses that relate both the response variables characterizing bacterial breakthrough curves and the bacterial transport parameters to the measurements of sediment characteristics. In agreement with colloid–filtration theory, %ER, C_{max}/C_0, and R_C were positively and k_c was negatively correlated to d_{50}. R_C was also positively correlated to MB. Greater autochthonous microbial biomass resulted in allochthonous bacteria moving through the core more conservatively, possibly the result of attachment sites being occupied by the indigenous microbial community.

Previous studies have indicated that under certain conditions, sediment physical properties were more important factors than chemical properties. Dong et al. (2002) concluded that for their intact cores, bacterial retention was dominated by grain size as opposed to the degree of metal hydroxide coatings for the adhesion-deficient bacterial strain used. Fontes et al. (1991) concluded that transport of a gram-negative coccus and a gram-negative rod (both approximately 0.75 mm in diameter) was more strongly affected by sediment grain size than the solution ionic strength or the type of organism. The results of the regression analyses performed here suggest that when groundwater chemistry and type of bacteria are held constant, bacterial transport through natural aquifer sediments is largely controlled by the sediment characteristics pertaining to the grain size distribution (primarily the d_{50} and secondarily C_u) and K. As predicted by colloid–filtration theory, most of the core-to-core variability associated with %ER and C_{max}/C_0 (88 and 76%, respectively) was explained by d_{50} alone. Similarly, Fontes et al. (1991) found that the %ER and C_{max}/C_0 were most dependent on grain size (increasing with increasing grain size). They also found effluent ionic strength and the average cell size (factors held constant in the current study) were secondary factors. Dong et al. (2002) also found an inverse relationship between the median grain size and the fraction of bacteria retained within cores. The dependence of T_{peak} on C_u (and K) indicates that bacterial breakthrough is affected by the degree of heterogeneity within the sediments; therefore, bacterial transport predictions based on column experiments using sieved and sorted sediments should be made with caution.

The regression models developed in this study have the potential to be used as predictive tools, especially because they are based on easily-measurable sediment characteristics. To predict advection and dispersion, appropriate effective porosity and dispersivity values must be estimated. When estimating the effective porosity for bacterial transport, conservative-tracer experiments are not appropriate. Instead, for the sediment type represented in these experiments, an appropriate value can be estimated from hydraulic conductivity and the sand content, as together they account for 66% of the core-to-core variability associated with the effective porosity value. Dispersivity values, conversely, are not significantly different from those associated with bromide transport; therefore, they can be estimated from conservative-tracer experiments. Alternatively, they can be estimated from C_u or d_{50}, which accounted for 44 and 61% of the core-to-core variability in dispersivity, respectively.

Other parameters crucial to predict bacterial transport are the attachment- and detachment-rate coefficients. As previously found (Fontes et al., 1991; Hornberger et al., 1992; Dong et al., 2002),

the degree of attachment increased as the median grain size decreased. Hornberger et al. (1992) also determined that k_c was higher with larger cell size and higher solution ionic strength (not considered in this study). We developed two regression models to predict k_c. One, based on d_{50}, accounted for 61% of the inter-core variability while the other, based on K and C_u, accounted for 89% of the observed core-to-core variability. While the relationship to the median grain size and, therefore, hydraulic conductivity is predicted by colloid–filtration theory, the specific relationship to sorting is unexpected. That relationship does, however, support the notion that heterogeneities in grain size distribution "may be responsible for much of the long-range transport of microbes" (Fontes et al., 1991). We hypothesis the relationship of the attachment-rate coefficient to the uniformity coefficient results from greater preferential flow in less uniform sediment exposing bacteria to less sediment surface area.

Estimation of the detachment-rate coefficient has been largely ignored in previous studies despite the fact that non-equilibrium detachment can result in bacterial transport much farther than one would predict assuming irreversible attachment. The detachment-rate coefficient largely controls the long-term tail concentration of the modeled breakthrough curves. Regression analysis indicated that k_y-values can be predicted based on median grain size, organic-matter content and the effective porosity for bacteria which together explained 76% of the observed variability; detachment occurred more readily with larger grain sizes, greater effective porosity and in the presence of greater amounts of organic-matter. It is possible that with more negatively charged organic coatings, bacterial attachment is weakened. More experiments are needed to further investigate these relationships. The problem with this model for k_y or the alternative model in Table 10, equation xiii, is that they are both dependent on an estimate of the effective porosity for the bacteria which is a difficult parameter to obtain. The regression models could be used in conjunction with regression models for the bacterial transport effective porosity based on sediment characteristics (Table 10, equations vi or vii), although this procedure does add additional uncertainty to the process.

Percent fines (silt plus clay) and total porosity were found to be relatively unimportant for these glacial-outwash sediments and experimental conditions. There was considerable core-to-core variability in microbial biomass, yet only R_C was found to be significantly related to biomass. The lack of a relationship between biomass and k_c or k_y indicated that the degree to which attachment sites were already occupied with indigenous bacteria may not have been a very important factor in these experiments. Microbial biomass was determined by sampling sediment just above and below each 10-cm long core so as not to disturb the core itself. There was substantial variability between the top and bottom measurements suggesting substantial variability in biomass within each core. The average of the two measurements was used in regression analyses, and it is possible that average biomass did not accurately reflect biomass within the core. Therefore, it is possible that the autochthonous microbial community is important to allochthonous bacterial transport as suggested by the regression model for R_C.

While the majority of the model parameter variability has been accounted for, the mineralogy of the sediments (e.g., degree of metal-oxyhydroxide coatings) was not determined and may account for some of the variability in the breakthrough curves and model parameter values. The sign and magnitude of the mineral surface charge affect bacterial attachment (Knapp et al., 1998). Bacteria are usually negatively charged and tend to attach to positively-charged metal-oxyhydroxide coatings more readily than they do quartz surfaces. Knapp et al. (1998) found that relatively small amounts of iron-oxyhydroxide coatings on quartz sand grains had a "profound effect on the transport of bacteria." Conversely, Dong et al. (2002) concluded sediment physical properties were more important than the degree of metal-oxyhydroxide coatings. More

experiments in different environments are needed to determine the relative importance of the mineralogy versus grain size distribution with respect to transport of *E. coli* and other bacteria.

4.6. Comparison of regression approach and use of colloid–filtration theory

This study presents an alternative to using colloid–filtration theory in lieu of running bacterial transport experiments − using sediment characteristics and regression relationships to estimate model parameter values. The regression model for the attachment-rate coefficient accounts for a much greater proportion of the observed variability of the CXTFIT-calibrated values than does the colloid–filtration theory applied without the benefit of bacterial transport experiments. The regression models also allow estimation of other necessary model parameters (detachment-rate coefficient, bacterial pore-water velocity and dispersivity). For these reasons, the regression approach has the potential to out-perform the colloid–filtration theory. More transport experiments are required, however, to test how well it can perform on cores not used in development of the regression models. The regression approach is also limited in other ways. The regression models were developed for a limited range of experimental conditions and a set of relatively short cores. The approach does not take into account variability of bacterial size and morphology, groundwater chemistry (including temperature and ionic strength), degree of metal-oxyhydroxide coatings, temporal and spatial variability of sticking efficiencies and the possibility of entrapped air in the core. More investigation is needed to determine whether the predictions will work well at scales larger than those used in this study (10 cm) and for different flow rates, different bacterial-pulse concentrations and widths, different temperatures, different ionic strengths and a wider range of sediment types.

5. Conclusions

Bacterial transport through laboratory cores of intact, glacial-outwash aquifer sediment was investigated with the overall goal of better understanding bacterial transport and developing a predictive capability based on the sediment characteristics. Few previous studies have been conducted on intact natural material and most of those studies have used more homogeneous material (Bolster et al., 1999; Fuller et al., 2000; Dong et al., 2002). The principal findings of the study were:

- Bacterial transport varied greatly among the cores. Maximum concentrations normalized to the input concentrations ranged from 5.4×10^{-7} to 0.36 and effluent recoveries ranged from 2.9×10^{-4} to 59%.
- Bacterial breakthrough was generally rapid with a sharp peak occurring earlier than the bromide peak, on average, by a factor of 1.9. Modeled bacterial velocities were significantly higher than those for bromide. Subsequently, the bacterial effective porosities were, on average, 0.53 times those for bromide. These results indicated that estimates of velocity and effective porosity based on conservative-tracer transport should not be used when predicting bacterial transport. Bacterial dispersivity values, on the other hand, were not significantly different from those for bromide.
- Bacterial breakthroughs exhibited long tails of relatively constant concentration averaging three orders of magnitude less than the peak concentration for up to 32 pore volumes. The tails were consistent with non-equilibrium detachment. This conclusion was corroborated by the results of six flow-interruption experiments in which the flow through the cores was stopped for 24 h and then resumed. Upon resumption, bacterial concentrations in the effluent increased an average of 6.1 times, indicating kinetic detachment.

- Bacterial breakthrough in 14 of the cores was accurately simulated with a CXTFIT transport model incorporating advection, dispersion and first-order kinetic attachment/detachment. Other more complex models that included additional equilibrium attachment/detachment and pseudo-first-order decay did not significantly improve the model fits. Model efficiencies ranged from 0.65 to 1.0 and averaged 0.92.
- Multiple regression analyses were used to explore the relationships between bacterial transport and sediment characteristics. The degree of differential advection between bromide and bacteria was inversely proportional to the median grain size, indicative of pore-size exclusion. The peak bacterial concentrations arrived more quickly in cores that had lower hydraulic conductivities and were more poorly sorted. As predicted by colloid–filtration theory, more effluent bacteria were recovered in cores with larger median grain size.
- Regression analysis also quantified relations among calibrated model parameter values and easily-measurable sediment characteristics: median grain size, degree of sorting, sand content, organic-matter content and hydraulic conductivity. These properties accounted for 66%, 61% and 89% of the core-to-core variability in the bacterial effective porosity, dispersivity and attachment-rate coefficient, respectively. In addition, the bacterial effective porosity, median grain size and organic-matter content accounted for 76% of the inter-core variability in the detachment-rate coefficient. The resulting regression equations potentially allow prediction of bacterial transport based on sediment characteristics and are an alternative to using the colloid–filtration theory.
- When colloid–filtration theory was used with the calibrated bacterial velocities and in conjunction with the core retention data to estimate the collision efficiency, it accurately captured the core-to-core variability of the calibrated attachment-rate coefficients (R^2-adj = 0.92). This led to accurate estimates of the peak concentration and its arrival time. The long tail observed in bacterial breakthrough curves, however,(a function of kinetic detachment) was not accounted for by colloid–filtration theory.
- Colloid–filtration theory, applied without the benefit of running bacterial transport experiments (i.e., without retention data and without knowing the average bacterial velocity), accounted for only about 28% of the observed core-to-core variability in CXTFIT-calibrated k_c values. In contrast, the regression model shown in Table 10, equation xi, accounted for 89% of the observed variability. Forward CXTFIT simulations using k_c values predicted by colloid–filtration theory tended to underestimate peak bacterial concentration and overestimate its arrival time.

Notation

A_s	Happel correction factor
c	Contaminant concentration in liquid phase [CFU L^{-3}]
%C	Percent clay content
c_{avg}	Average of the observed bacterial, effluent concentrations [CFU L^{-3}]
c_i	ith observed bacterial, effluent concentration [CFU L^{-3}]
c_{im}	Solute concentration in the immobile portion of the pore space [$M\,L^{-3}$]
c_m	Solute concentration in the mobile portion of the pore space [$M\,L^{-3}$]
CFU	Colony-forming unit
C_{max}/C_0	Maximum effluent concentration normalized to the input concentration
C_u	Uniformity coefficient = d_{60}/d_{10}
D	Dispersion coefficient [$L^2\ T^{-1}$]
D_m	Dispersion coefficient in the mobile portion of the pore space [$L^2\ T^{-1}$]
d_{10}	Grain size for which 10% of the sediment is finer by weight [L]
d_{17}	Grain size for which 17% of the sediment is finer by weight [L]

d_{50}	Median grain size [L]
d_{60}	Grain size for which 60% of the sediment is finer by weight [L]
d_c	Diameter of grains of transport medium [L]
d_p	Diameter of bacteria [L]
E	Model efficiency
%ER	Percentage of input bacteria measured in the effluent during first 20 h of the experiments
f	Two-site model parameter, fraction of exchange sites that are always at equilibrium
%G	Percent gravel content
k	Boltzman constant [$M\,L^2T^{-2}K^{-1}$]
K	Hydraulic conductivity [L/T]
K_d	Equilibrium sorption coefficient $=\theta k_f/(\rho_b k_r)$ [$M^{-1}L^3$]
k_c	Forward sorption or attachment-rate coefficient [T^{-1}]
k_{str}	Straining coefficient [T^{-1}]
k_y	Backward sorption or entrainment rate coefficient [T^{-1}]
L	Core length [L]
MB	Total microbial biomass [$nmol\ M^{-1}$]
MSC	Model selection criterion
n	Number of model observations
N_G	Colloid filtration theory gravitation number
N_{Lo}	Colloid filtration theory London-van der Walls number
N_{Pe}	Colloid filtration theory Peclet number
N_R	Colloid filtration theory interception number
OM	Organic-matter content
p	Number of model fitting parameters
R	Retardation factor
R_C	Ratio of the bacterial to bromide normalized peak concentration
r_i	ith residual between model prediction and observation
R_N	Fraction of bacteria retained in the core
R_T	Ratio of the bacterial to bromide and peak arrival times in pore volumes
s	Contaminant concentration in adsorbed phase [$M\,M^{-1}$]
%S	Percent sand content
%Si	Percent silt content
t	Time [T]
T	Temperature [K]
T_{peak}	Time of the peak arrival expressed in pore volumes
%TR	Total bacterial recovery from effluent (first 20 h) and attached to sediment
v	Flow velocity [$L\ T^{-1}$]
v_m	Pore-water velocity through the mobile portion of the pore space [$L\ T^{-1}$],
x	Distance from core inlet or source [L]
α	Sticking or collision efficiency
α_L	Dispersivity [L]
β	Ratio of the mobile region porosity to the total porosity
η	Single-collector efficiency
η_{sg}	Straining parameter
ρ_b	Sediment bulk density [$M\,L^{-3}$]
ρ_f	Fluid density [$M\,L^{-3}$]
ρ_p	Bacterial density [$M\,L^{-3}$]

θ Porosity of the transport medium for saturated sediment
θ_e Effective porosity for bacteria
θ_m Effective porosity for bromide
ω Mass-transfer coefficient

Acknowledgement

This study was supported by grants from the National Institutes for Water Resources together with the United States Geological Survey, the City of Cincinnati Water Works in conjunction with the Ohio Water Development Authority and internal grants from Miami University. Thanks to Rodney Kolb formerly with Miami University's Instrumentation Laboratory for his help in the design of column apparatus.

References

Bitton, G., Harvey, R.W., 1992. Transport of pathogens through soils and aquifers. In: Mitchell, R. (Ed.), Environmental Microbiology. Wiley-Liss, Inc., New York.

Bolster, C.H., Herman, J.S., Hornberger, G.M., Mills, A.L., 1999. Spatial distribution of deposited bacteria following miscible displacement experiments in intact cores. Water Resour. Res. 35 (6), 1797–1807.

Bolster, C.H., Mills, A.L., Hornberger, G.M., Herman, J.S., 2000. Effect of intra-population variability on the long-distance transport of bacteria. Ground Water 38 (3), 370–375.

Bolster, C.H., Mills, A.L., Hornberger, G.M., Herman, J.S., 2001. Effect of surface coatings, grain size and ionic strength on the maximum attainable coverage of bacteria on sand surfaces. J. Contam. Hydrol. 50, 287–305.

Bradford, S.A., Simunek, J., Bettahar, M., van Genuchten, M.t., Yates, S.R., 2003. Modeling colloid attachment, straining, and exclusion in saturated porous media. Environ. Sci. Technol. 37 (10), 2242–2250.

Brady, N.C., 1974. The Nature and Properties of Soils, 8th ed. MacMillan Publishing Co., Inc., New York.

Brusseau, M.L., Hu, Q., Srivastava, R., 1997. Using flow interruption to identify factors causing nonideal contaminant transport. J. Contam. Hydrol. 24, 205–219.

Chatterjee, S., Price, B., 1977. Regression Analysis by Example. John Wiley & Sons, New York.

Corapcioglu, M.Y., Haridas, A., 1984. Transport and fate of microorganisms in porous media: a theoretical investigation. J. Hydrol. 72, 149–169.

Craun, G.F., Calderon, R.L., 1997. Microbial risks in groundwater systems: epidemiology of waterborne outbreaks. Paper Presented at the Groundwater Foundation's 12th Annual Fall Symposium: Under the Microscope: Examining Microbes in Groundwater, American Water Works Association Research Foundation, Denver, Colorado.

Dong, H., Onstott, T.C., DeFlaun, M.F., Fuller, M.E., Scheibe, T.D., Streger, S.H., Rothmel, R.K., Mailloux, B.J., 2002. Relative dominance of physical versus chemical effects on the transport of adhesion-deficient bacteria in intact cores from South Oyster, Virginia. Environ. Sci. Technol. 36 (5), 891–900.

Fetter, C.W., 1999. Contaminant Hydrogeology, Second ed. Prentice Hall, Upper Saddle River, NJ.

Fetter, C.W., 2001. Applied Hydrogeology, Fourth ed. Prentice Hall, Upper Saddle River, NJ.

Findlay, R.H., 2004. Determination of microbial community structure using phospholipid fatty acid profiles, In: Kowalchuk, G.A., De Bruijn, F.J., Head, I.M., Akkermans, A.D.L., van Elsas, J.D. (Eds.), Second ed. Molecular Microbial Ecology Manual, vol. 4.08. Kluwer Academic Publishers, Dordrecht, The Netherlands, pp. 983–1004.

Findlay, R.H., King, G.M., Watling, L., 1989. Efficacy of phospholipid analysis in determining microbial biomass in sediments. Appl. Environ. Microbiol. 54, 2888–2893.

Fontes, D.E., Mills, A.L., Hornberger, G.M., Herman, J.S., 1991. Physical and chemical factors influencing transport of microorganisms through porous media. Appl. Environ. Microbiol. 57 (9), 2473–2481.

Foppen, J.W.A., Mporokoso, A., Schijven, J.F., 2005. Determining straining of *Escherichia coli* from breakthrough curves. J. Contam. Hydrol. 76, 191–210.

Fuller, M.E., Dong, H., Mailloux, B.J., Onstott, T.C., 2000. Examining bacterial transport in intact cores from Oyster, Virginia: effect of sedimentary facies type on bacterial breakthrough and retention. Water Resour. Res. 36 (9), 2417–2431.

Gerba, C.P., Bitton, G., 1984. In: Bitton, G., Gerba, C.P. (Eds.), Microbial Pollutants: Their Survival and Transport Pattern to Groundwater. Groundwater Pollution Microbiology. John Wiley & Sons, New York.

Gerba, C.P., Yates, M.V., Yates, S.R., 1991. In: Hurst, C.J. (Ed.), Quantification of Factors Controlling Viral and Bacterial Transport in the Subsurface. Modeling the Environmental Fate of Microorganisms. American Society for Microbiology, Washington, DC.

Gross, M.J., Logan, B.E., 1995. Influence of different chemical treatment on transport of *Alcaligenes paradoxus* in porous media. Appl. Environ. Microbiol. 61 (5), 1750–1756.

Harvey, R.W., 1991. In: Hurst, C.J. (Ed.), Parameters Involved in Modeling Movement of Bacteria in Groundwater. Modeling the Environmental Fate of Microorganisms. American Society for Microbiology, Washington, DC.

Harvey, R.W., 1997. In: Hurst, C.J., Knudsen, G.R., McInerney, J.J., Stetzenback, L.D., Walter, M.V. (Eds.), In Situ and Laboratory Methods to Study Subsurface Microbial Transport. Manual of Environmental Microbiology. ASM Press, Washington, DC.

Harvey, R.W., Garabedian, S.P., 1991. Use of colloid filtration theory in modeling movement of bacteria through a contaminated sandy aquifer. Environ. Sci. Technol. 25 (1), 178–185.

Harvey, R.W., Aronson, D.E., Barber II, L.B., Garabedian, S.P., Metge, D.W., Scholl, M.A., Smith, R.L., 1991. The role of physical and chemical heterogeneity in the interpretation of small-scale tracer tests involving microorganisms. Water-Resources Investigations, U.S. Geological Survey WRI 91-4034.

Harvey, R.W., Kinner, N.E., MacDonald, D., Metge, D.W., Bunn, A., 1993. Role of physical heterogeneity in the interpretation of small-scale laboratory and field observations of bacteria, microbial-sized microsphere, and bromide transport through aquifer sediments. Water Resour. Res. 29 (8), 2713–2721.

Harvey, R.W., Kinner, N.E., Bunn, K.A., MacDonald, D., Metge, D.W., 1995. Transport behavior of groundwater protozoa and protozoan-sized microspheres in sandy aquifer sediments. Appl. Environ. Microbiol. 61 (1), 209–217.

Harvey, R.W., Metge, D.W., Kinner, N., Mayberry, N., 1997. Physiological consideration in applying laboratory-determined buoyant densities to predictions of bacterial and protozoan transport in groundwater: results of in-situ and laboratory tests. Environ. Sci. Technol. 31 (1), 289–295.

Hendry, M.J., Lawrence, J.R., Maloszewski, P., 1999. Effect of velocity on the transport of two bacteria through saturated sand. Ground Water 37 (1), 101–112.

Hornberger, G.M., Mills, A.L., Herman, J.S., 1992. Bacterial transport in porous media: evaluation of a model using laboratory observations. Water Resour. Res. 28 (3), 915–938.

Huyysman, F., Verstraete, W., 1993. Water-facilitated transport of bacteria in unsaturated soil columns: influence of cell surface hydrophobicity and soil properties. Soil Biol. Biochem. 25 (1), 83–90.

Jewett, D.G., Hilbert, T.A., Logan, B.E., Arnold, R.G., Bales, R.C., 1995. Bacterial transport in laboratory columns and filters: influence of ionic strength and pH on collision efficiency. Water Res. 29 (7), 1673–1680.

Johnson, W.P., Logan, B.E., 1996. Enhanced transport of bacteria in porous media by sediment-phase and aqueous-phase natural organic matter. Water Res. 30 (4), 923–931.

Johnson, W.P., Blue, K.A., Logan, B.E., Arnold, R.G., 1995. Modeling bacterial detachment during transport through porous media as a residence-time-dependent process. Water Resour. Res. 31 (11), 2649–2658.

Knapp, E.P., Herman, J.S., Hornberger, G.M., Mills, A.L., 1998. The effect of distribution of iron-oxyhydroxide grain coatings on the transport of bacterial cells in porous media. Environ. Geol. 33 (4), 243–248.

Logan, B.E., Jewett, D.G., Arnold, R.G., Bouwer, E.J., O'Melia, C.R., 1995. Clarification of clean-bed filtration models. J. Environ. Eng. 121 (12), 869–873.

Macler, B.A., Merkle, J.C., 2000. Current knowledge on groundwater microbial pathogens and their control. Hydrogeol. J. 8, 29–40.

Martin, R.E., Bouwer, E.J., Hanna, L.M., 1992. Applications of clean-bed filtration theory to bacterial deposition in porous media. Environ. Sci. Technol. 26, 1053–1058.

Matthess, G., Pekdeger, A., 1985. In: Ward, C.H., Giger, W., McCarty, P.L. (Eds.), Survival and Transport of Pathogenic Bacteria and Viruses in Ground Water. Ground Water Quality. John Wiley, New York.

McCaulou, D.R., Bales, R.C., McCarthy, J.F., 1994. Use of short-pulse experiments to study bacteria transport through porous media. J. Contam. Hydrol. 15, 1–14.

McCaulou, D.R., Bales, R.C., Arnold, R.G., 1995. Effect of temperature-controlled motility on transport of bacteria and microspheres through saturated sediment. Water Resour. Res. 31 (2), 271–280.

Mills, A.L., Herman, J.S., Hornberger, G.M., DeJesus, T.H., 1994. Effect of solution ionic strength and iron coatings on mineral grains on the sorption of bacterial cells to quartz sand. Appl. Environ. Microbiol. 60, 3300–3306.

Morley, L.M., Hornberger, G.M., Mills, A.L., Herman, J.S., 1998. Effect of transverse mixing on transport of bacteria through heterogeneous porous media. Water Resour. Res. 34 (8), 1901–1908.

Nkedi-Kizza, P., Bigger, J.W., Selim, H.M., van Genuchten, M.Th., Wierenga, P.J., Davidson, J.M., Nielsen, D.R., 1984. On the equivalence of two conceptual models for describing ion exchange during transport through an aggregated oxisol. Water Resour. Res. 20 (8), 1123–1130.

Peterson, T.C., Ward, R.C., 1989. Development of a bacterial transport model for coarse soils. Water Resour. Bull. 25 (2), 349–357.

Rajagopalan, R., Tien, C., 1976. Trajectory analysis of deep-bed filtration with the sphere-in-a-cell porous media model. AIChE J. 28, 523–533.

Saiers, J.E., Hornberger, G.M., Liang, L., 1994. First- and second-order kinetics approaches for modeling the transport of colloidal particles in porous media. Water Resour. Res. 30 (9), 2499–2506.

Scholl, M.A., Harvey, R.W., 1992. Laboratory investigations on the role of sediment surfaces and groundwater chemistry in transport of bacteria through a contaminated sandy aquifer. Environ. Sci. Technol. 26 (7), 1410–1417.

Scholl, M.A., Mills, A.L., Herman, J.S., Hornberger, G.M., 1991. The influence of mineralogy and solution chemistry on attachment of bacteria to representative aquifer materials. J. Contam. Hydrol. 6, 331–336.

Schulte, E.E., 1996. In: Hanlon Jr., E.A., Hopkins, B.G., Tabatabai, M.A. (Eds.), Estimation of Soil Organic Matter by Weight Loss-on-Ignition. SSSA Special Publication, vol. 46. Soil Science Society of America, Madison, WI.

Smith, M.S., Thomas, G.W., White, R.E., Ritonga, C., 1985. Transport of *Escherichia coli* through intact and disturbed soil columns. J. Environ. Qual. 14 (1), 87–91.

Tan, Y., Gannon, J.T., Baveye, P., Alexander, M., 1994. Transport of bacteria in an aquifer sand: experiments and model simulations. Water Resour. Res. 30 (12), 3243–3252.

Tien, C., Turian, R.M., Pandse, H., 1979. Simulation of deep bed filters. AIChE J. 25, 385–395.

Toride, N., Leij, F.J., van Genuchten, M.Th., 1995. The CXTFIT code for estimating transport parameters from laboratory or field tracer experiments, version 2.0. Research Report, vol. 137. US Salinity Laboratory, Agricultural Research Service, US Department of Agriculture, Riverside, CA.

van Genuchten, M.Th., Wagenet, R.J., 1989. Two-site/two-region models for pesticide transport and degradation: theoretical development and analytical solutions. Soil Sci. Soc. Am. J. 53, 1303–1310.

Webb, E.K., Anderson, M.P., 1996. Simulation of preferential flow in three-dimensional heterogeneous conductivity fields with realistic internal structure. Water Resour. Res. 32 (3), 533–545.

Weiss, T.H., Mills, A.L., Hornberger, G.M., Herman, J.S., 1995. Effect of bacterial cell shape on transport of bacteria in porous media. Environ. Sci. Technol. 29 (7), 1737–1740.